

We are IntechOpen, the world's leading publisher of Open Access books Built by scientists, for scientists

4,800

Open access books available

122,000

International authors and editors

135M

Downloads

Our authors are among the

154

Countries delivered to

TOP 1%

most cited scientists

12.2%

Contributors from top 500 universities



WEB OF SCIENCE™

Selection of our books indexed in the Book Citation Index
in Web of Science™ Core Collection (BKCI)

Interested in publishing with us?
Contact book.department@intechopen.com

Numbers displayed above are based on latest data collected.

For more information visit www.intechopen.com



Metrology for non-stationary dynamic measurements

Jan Peter Hessling

Measurement Technology, SP Technical Research Institute of Sweden

1. Introduction

The widely applied framework for calibrating measurement systems is described in the GUM - The Guide to the Expression of Uncertainty in Measurements (ISO GUM, 1993). Despite its claimed generality, it is evident that this guide focuses on measurements of stationary quantities described by any finite set of constant parameters, such as any constant or harmonic signal. Non-stationary measurements are nevertheless ubiquitous in modern science and technology. An expected non-trivial unique time-dependence, as for instance in any type of crash test, is often the *primary* reason to perform a measurement. Many formulations of the guide are indeed difficult to interpret in a dynamic context. For instance, correction and uncertainty are referred to as being *universal constant* quantities for *direct* interpretation. These claims cease to be true for non-stationary dynamic measurements.

A measurement is here defined as stationary if a time-independent parameterization of the quantity of interest is used. The classification is thus relative, and ultimately depends on personal ability and taste. A given measurement may be stationary in one context but not in another. Static and stationary measurements can be analysed similarly (ISO GUM, 1993) since constant parameters are used in both cases.

The term 'dynamic' is frequently used, but with rather different meanings. The use of the term 'dynamic measurement' is often misleading as it normally refers to the mere time-dependence, which itself never requires a dynamic analysis. Instead, the classification into a dynamic or static measurement that will be adopted refers to the relation between the system and the signal: "The key feature that distinguishes a dynamic from a static measurement is the speed of response (bandwidth) of the measurement systems as compared to the speed at which the measured signal is changing" (Esward, 2009, p. 1).

This definition indirectly involves the acceptable accuracy through the concept of response time or bandwidth. In this formulation, a dynamic responds much slower than a static measurement system and therefore needs a dynamic rather than a static analysis. The relativity between the system and the signal is crucial - no signal or system can be 'dynamic' on its own. A static analysis is often sufficient whether it refers to a measurement of a constant, stationary or non-stationary time-dependent quantity. Indirectly and misleadingly the guide (ISO GUM, 1993) indicates that this is always the case. This is apparent from the lack of discussion of e.g. differential or difference model equations, time delay, temporal correlations and distortion. The difference between ensemble and time averages is not mentioned, but is very important for non-stationary non-ergodic measurements.

Even strongly imprecise statements of measurement uncertainty may in practice have limited consequences. It may be exceedingly difficult to even illustrate an incorrect analysis due to neglect or erroneous treatment of dynamic effects. Dynamic artefacts or fundamental physical signals corresponding to fundamental constants like the unit of electric charge do not exist. These aspects are probably the cause to why dynamic analysis still has not penetrated the field of metrology to the same extent as in many other related fields of science and engineering. By limiting the calibration services to only include characterizations and not provide methods or means to translate this information to the more complex targeted measurement, the precious calibration information can often not be utilized at all (!) to assess the quality of the targeted measurement. The framework Dynamic Metrology presented in this chapter is devoted to bridge this gap from a holistic point of view. The discussion will focus on concepts from a broad perspective, rather than details of various applications. Referencing will be sparse. For a comprehensive exploration and list of references the reader is advised to study the original articles (Hessling, 2006; 2008a-b; 2009a), which provide the basis of Dynamic Metrology.

2. Generic aspects of non-stationary dynamic measurements

The allowed measurement uncertainty enters into the classification of dynamic measurements through the definitions of response time of the system and change of rate of possible signals. This is plausible since the choice of tools and analysis (static/stationary or dynamic) is determined by the acceptable accuracy.

As recognized a long time ago by the novel work of Wiener in radar applications (Wiener, 1949), efficient dynamic correction will always involve a subtle balance between reduction of systematic measurement errors and unwanted amplification of measurement noise. How these contributions to the measurement uncertainty combines and changes with the degree of correction is therefore essential. The central and complex role of the dynamic measurement uncertainty *in* the correction contrasts the present stationary treatment.

Interactions are much more complex in non-stationary than in stationary measurements. Therefore, engineering fields such as microwave applications and high speed electronics dedicated to dynamic analysis have taken a genuinely system-oriented approach. As microwave specialists know very well, even the simplest piece of material needs careful attention as it may require a full dynamic specification. This has profound consequences. Calibration of only vital parts (like sensors) might not be feasible as it only describes one ingredient of a complex dynamic 'soup'. Its taste may depend on all ingredients, but also on how it is assembled and served. Testing the soup in the relevant environment may be required. Sometimes the calibration procedures have to leave the lab (*in vitro*) and instead take place under identical conditions to the targeted measurements (*in situ*).

The relativity between signal and system has practical consequences for *every* measurement. Repeated experiments will result in different signals and hence different performance. The dynamic correction will be unique and must be re-calculated for every measured signal. There will thus never be universal dynamic corrections for non-stationary measurements, as can be found for stationary measurements in a calibration laboratory.

The need for repeated *in situ* evaluation illustrates the pertinent and critical aspect of transferability of the calibration result. This is seldom an issue for stationary calibration methods where a limited set of universal numbers is sufficient to describe the result.

Stationary measurements have minute variations in comparison to the enormous freedom of non-stationary events. Physical generation of *all* possible non-stationary signals in calibrations will always be an insurmountable challenge. Indirect analyses based on uncertain and potentially abstract dynamic models are required. In turn, these models are deduced from limited but nevertheless, for the purpose complete testing against references. This testing is usually referred to as 'dynamic calibration' while the model extraction is denoted 'system identification'. Here calibration will be associated to the *combined* operation of testing and model identification. The testing operation will be called 'characterization'.

The performance of the targeted non-stationary measurements will be assessed with calculations using measured signals and an uncertain *indirect* model of the measurement. Essentially, the intermediate stage of modelling reduces the false appearance of extremely complex measurements due to the high dimensionality of the *signals* (directly observable) to the true much lower complexity of the measurement described by the *systems* (indirectly observable). It is the indirect modelling that makes the non-stationary dynamic analysis of measurements possible.

The measurand is often a function of a signal rather than a measurable time-dependent quantity of any kind. The measurand could be the rise time of oscilloscopes, the vibration dose R for adverse health effects for whole body vibrations, complex quantities such as the error vector magnitude (EVM) of WCDMA signals in mobile telecommunication (Humphreys & Dickerson, 2007), or power quality measures such as 'light flicker' (Hessling, 1999). Usually these indexes depend on time-dependent signals and do not provide complete information. A complete analysis of signals and systems is required to build a traceability chain from which the measurands can be estimated at any stage. As illustrated in Fig. 1, the measurement uncertainty is first propagated from the characterization to the model, from the model to the targeted measurement, and perhaps one step further to the measurand. The final step will not be addressed here since it is application-specific without general procedures. Fortunately, the propagation is straight-forward using the definition of the measurand often described in detail in standards (for the examples mentioned in this paragraph, EA-10/07, ISO 2631-5, 3GPP TS, IEC 61000-4-15).

The analysis of non-stationary dynamic measurements generally requires strongly interacting dynamic models. In situ calibrations of large complex systems as well as repeated in situ evaluations for every measurement may be needed. The uncertainty must be propagated in two or more stages. Realized in full, this requires nothing less than a new paradigm to be introduced in measurement science.

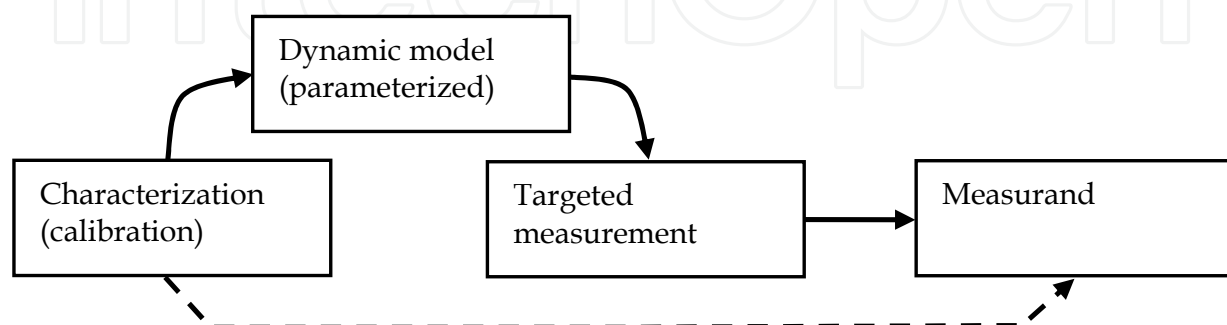


Fig. 1. Propagation (arrows) of non-stationary (full) measurement uncertainty compared to the conventional stationary case (ISO GUM, 1993) (dashed).

3. State-of-the-art dynamic analysis

The level of applications of dynamic analyses varies greatly. Leading manufacturers of measurement equipment are often well ahead of measurement science, as the realization of dynamic operations is facilitated by detailed product knowledge. However, dynamic design usually requires a substantial amount of compromises. Maximal bandwidth or slew-rate may for instance be incompatible with good time domain performance. A neutral evaluation in terms of an extended calibration service is strongly needed. Nevertheless, in many cases the motivation is low, as the de-facto standards of calibration are restricted and simplified. The motivation should primarily originate from end-users. The field of dynamic analysis in the context of calibration, or waveform metrology, is currently emerging at major national metrology institutes in a number of applications. This is the precursor for changing calibration standards and procedures to better account for the experimental reality.

The development of calibration of accelerometers illuminates the progress. One part of a present standard (ISO 16063, 2001) is based on the shock sensitivity of accelerometers. The calibration has suffered from poor repeatability due to large overseen dynamic errors (Hessling, 2006) which depend on unspecified details of the pulse excitation. A complete specification would not solve the problem though, as the pulse would neither be possible to accurately realize in most calibration experiments, nor represent the variation of targeted measurements. Despite this deficiency, manufacturers have provided dynamic correction of accelerometers for many years (Bruel&Kjaer, 2006). The problem with the present shock calibration is now about to be resolved with an indirect analysis based on system identification, which also provides good transferability. The solution parallels the analysis to be proposed here. Beyond this standard, dynamic correction as well as uncertainty evaluation for this system has also recently been proposed (Elster et al., 2007).

Mechanical fatigue testing machines and electrical network analyzers are comparable, as they both have means for generating the excitation. Their principles of dynamic calibration are nonetheless different in almost all ways. For network analyzers, simple daily in situ calibrations with built-in software correction facilities are made by end-users using calibrated calibration kits. Testing machines usually have no built-in correction. Present dynamic calibration procedures (ASTM E 467-98a, 1998) are incomplete, direct and utilize calibration bars which are *not* calibrated. This procedure could be greatly improved if the methods of calibrating network analyzers would be transferred and adapted to mechanical testing machines.

The use of oscilloscopes is rapidly evolving. In the past they were used for simpler measurement tasks, typically detecting but not accurately quantifying events. With the advent of sampling oscilloscopes and modern signal processing the usage has changed dramatically. Modern sampling techniques and large storage capabilities now make it possible to accurately resolve and record various signals. Dynamic correction is sometimes applied by manufacturers of high performance oscilloscopes. Occasionally national laboratories correct for dynamic effects. A dissatisfying example is the standard (EA-10/07, 1997) for calibrating oscilloscopes by evaluating the rise time of their step response. Unfortunately, a scalar treatment of a non-stationary signal is prescribed. This results in the same type of calibration problem as for the shock sensitivity of accelerometers described above. The uncertainty of the rise time cannot even in principle be satisfactorily evaluated, as relevant distortions of the generated step are not taken into account. Further, interaction effects are not addressed, which is critical for an instrument that can be connected to a wide

range of different equipments. Correction is often synthesized taking only an approximate amplitude response into account (Hale & Clement, 2008). Neglecting the phase response in this way is equivalent to not knowing if an error should be removed by subtraction or addition! Important efforts are now made to account for such deficiencies (Dienstfrey et al., 2006; Williams et al., 2006). Many issues, such as how to include it in a standardized calibration scheme and transfer the result, remain to be resolved.

A general procedure of dynamic analysis in metrology remains to be formulated, perhaps as a dynamic supplement to the present guide (ISO GUM, 1993). As advanced dynamic modelling is currently *not* a part of present education curriculum in metrology, a substantial amount of user-friendly software needs to be developed. Most likely, the present calibration certificates must evolve into small dedicated computer programs which apply dynamic analysis to each measured signal and are synthesized and optimized according to the results of the calibration. In short, the infra-structure (methods and means) of an extended calibration service for dynamic non-stationary measurements needs to be built.

4. Dynamic Metrology – a framework for non-stationary dynamic analysis

In the context of calibration, the analysis of non-stationary dynamic measurements must be synthesized in a limited time frame without detailed knowledge of the system. In perspective of the vast variation of measurement systems and non-stationary signals, robustness and transferability are central aspects. There are many requirements to consider:

- **Generality:** Vastly different types of systems should be possible to model. These could be mechanical or electrical transducers, amplifiers, filters, signal processing, large and/or complex systems, hybrid systems etc.
- **Interactions:** Models of strong interactions between calibrated subsystems are often required to include all relevant influential effects.
- **Robustness:** There exists no limit regarding the complexity of the system. This requires low sensitivity to modelling and measurement errors etc.
- **In situ calibration and analysis:** Virtually all methods must be possible to transfer to common measurement computers and other types of computational hardware.
- **Transferability:** All results and methods must be formulated to enable almost fool-proof transfer to end-users without virtually any knowledge of dynamic analysis.

A framework (Dynamic Metrology) dedicated to analysis of dynamic measurements was recently proposed (Hessling, 2008b). All methods were based on standard signal processing operations easily packed in software modules. The task of repeated dynamic analysis for every measurement may effectively be distributed to three parties with different chores: Experts on Dynamic Metrology (1) derive general synthesis methods. These are applied by the calibrators (2) to determine dedicated but general software calibration certificates for the targeted measurement, using specific calibration information. The end users (3) apply these certificates to each measurement with a highly standardized and simple ['drag-and-drop'] implementation. Consequently, Dynamic Metrology involves software development on two levels. The calibrators as well as the end users need computational support, the former to *synthesize* (construct and adapt), the latter to *realize* (apply) the methods. For the steps of system identification, mathematical modelling and simulation reliable software packages are available. Such tools can be integrated with confidence into Dynamic Metrology. What

remains is to adapt and combine them into 'toolboxes' or modules for synthesis (calibrator) and realization (end-user), similar to what has been made for system identification (Kollár, 2003). This fairly complex structure is not a choice, but a consequence of; general goals of calibration, the application to non-stationary dynamic measurements and the fact that only the experts on Dynamic Metrology are assumed to have training in dynamic analysis.

Prototype methods for all present steps of analysis contained in Dynamic Metrology will be presented here. Dynamic characterization (section 4.1) provides the fundamental information about the measurement system. Using this information and parametric system identification (section 4.2), a dynamic model (section 4.2.1) with associated uncertainty (section 4.2.2) is obtained. From the dynamic model equation the systematic dynamic error can be estimated (section 4.3). The dynamic correction (section 4.4) is supposed to reduce this error by applying the optimal approximation to the inverse of the dynamic model equation. To evaluate the measurement uncertainty (section 4.5), the expression of measurement uncertainty (section 4.5.1) is derived from the dynamic model equation. For every uncertain parameter, a dynamic equation for its associated sensitivity is obtained. The sensitivities will be signals rather than numbers and can be realized using digital filtering, or any commercially available dynamic simulator (section 4.5.2). The discussion is concluded with an overview of all known limitations of the approach and expected future developments (section 4.6), and a summary (section 5). The versatility of the methods will be illustrated with a wide range of examples (steps of analysis given in parenthesis):

- Material testing machines (identification)
- Force measuring load cells (characterization, identification)
- Transducer systems for measuring force, acceleration or pressure (correction, measurement uncertainty – digital filtering)
- All-pass filters, electrical/digital (dynamic error)
- Oscilloscopes and related generators (characterization, identification, correction)
- Voltage dividers for high voltage (measurement uncertainty – simulations)

4.1 Characterization

The raw information of the measurement system required for the analysis is obtained from the characterization, where the measurement system is experimentally tested against a reference system. In perspective of the targeted measurement, the testing must be *complete*. All relevant properties of the system can then be transformed or derived from the results, but are not explicitly given. Using a *representation* in time, frequency or something else is only a matter of practical convenience (Pintelon & Schoukens, 2001). For instance, the bandwidth can be derived from a step response. The result consists of a numerical presentation with associated measurement uncertainty, strictly limited to the test signal(s). Different parts of the system can be characterized separately, provided the interactions can also be characterized. The simplest alternative is often to characterize whole assembled systems. When the environment affects the performance it is preferable to characterize the system in situ with a portable dynamic reference system. One example is the use of calibration kits for calibrating network analyzers. The accuracy of characterization of any subsystem should always be judged in comparison to the performance of the whole system. There is no point in knowing any link of a chain better than the chain as a whole.

How physical reference *systems* are realized is specific to each application. The test *signals* are however remarkably general. The test signals do not have to be non-stationary to be

used for analysis of non-stationary measurements. On the contrary, stationary signals generally give the highest accuracy. Usually there are important constraints on the relation between amplitude and speed of change/bandwidth of the signals. Harmonic sweeps generally yield the most accurate characterization, but test signals of high amplitude and high frequency may be difficult to generate and the testing procedure can be slow. Various kinds of impulses can be generated when stored mechanical, electric or magnetic energy is released. To control the spectrum of the signal frequency sweeps are superior, while high amplitude and sometimes high speed often requires the use of pulses. The design of excitation signals is important for the quality of modelling, and is thus an integral part of system identification (Pintelon & Schoukens, 2001).

The two mechanical examples will illustrate an in-vitro sensor and a corresponding in-situ system characterization. The non-trivial relation between them will be explored in section 4.2.3. The two electrical examples illustrate the duality of calibrating generators and oscilloscopes, or more generally, transmitters and receivers. The least is then characterized with the best performing instrument. The examples convey comparable dynamic information of the devices under test, but differently, with different accuracy and in different ranges. The often used impulse (h), step (v) and continuous $H(s = i2\pi f)$ or discrete time ($G(z = \exp(i2\pi f T_s))$, T_s sampling time) frequency (f) response characterizations are related via the Laplace- (L) and z-transform (Z), respectively,

$$h(t) = \frac{dv}{dt}, \quad \begin{matrix} G(z) = Z(h(t)) \\ H(s) = L(h(t)) \end{matrix} \quad (1)$$

Stationary sources of uncertainty (e.g. mass, temperature, pressure) are usually rather easy to estimate, but often provide minor contributions. For non-stationary test signals the largest sources of the uncertainty normally relate to the underlying time-dependent dynamic event. Typical examples are imbalances of a moving mechanical element or imperfections of electrical switching. All relevant sources of uncertainty must be estimated and propagated to the characterization result by detailed modelling of the experimental set up. The task of estimating the measurement uncertainty of the characterization is thus highly specialized and consequently not discussed in this general context. The uncertainty of the dynamic characterization is the fundamental 'seed' of unavoidable uncertainty, that later will be propagated through several steps as shown in Fig. 1 and combined with the uncertainty of the respective measurement (sections 4.2.2 and 4.5.1).

4.1.1 Example: Impulse response of load cell

An elementary example of characterization is a recent impulse characterization of a force measuring load cell displayed in Fig. 2 (left) (Hessling, 2008c, Appendix A). This force sensor is used in a material testing machine (Fig. 4, left). The load cell was hung up in a rope and hit with a heavy stiff hammer. As the duration of the pulse was estimated to be much less than the response time of the load cell, its shape could be approximated with an ideal Dirac-delta impulse. The equivalent force amplitude was unknown but of little interest: The static amplification of the load cell is more accurately determined from a static calibration. The resulting oscillating normalized impulse response is shown in Fig. 2 (right).

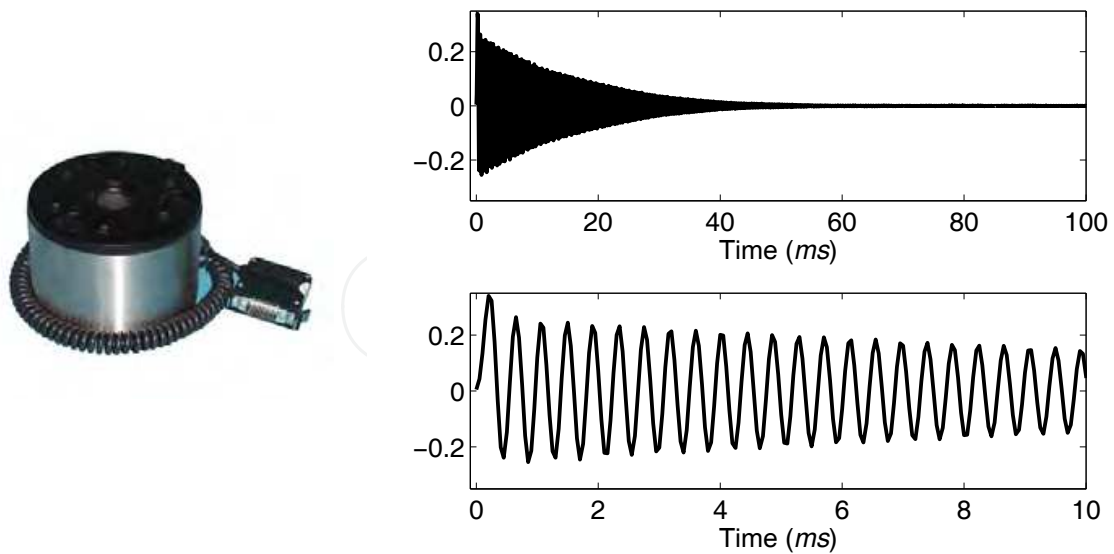


Fig. 2. Measured impulse response (right) of a load cell (left), on different time scales. The sampling rate is 20 kHz and the response is normalized to unit static amplification.

4.1.2 Example: Impulse response of oscilloscope and step response of generator

Oscilloscopes can be characterized with an optoelectronic sampling system (Clement et al., 2006). A short impulse is then typically generated from a 100-fs-long optical pulse of a pulsed laser, and converted to an electrical signal with a photodiode. A reference oscilloscope characterized with a reference optoelectronic sampling system may in turn be used to characterize step generators. Example raw measurements of a photodiode impulse and a step generator are illustrated in Fig. 3. A traceability chain can be built upon such repeated alternating characterizations of generators and oscilloscopes. If the measurand is the rise time it can be estimated from each characterization but not propagated with maintained traceability.

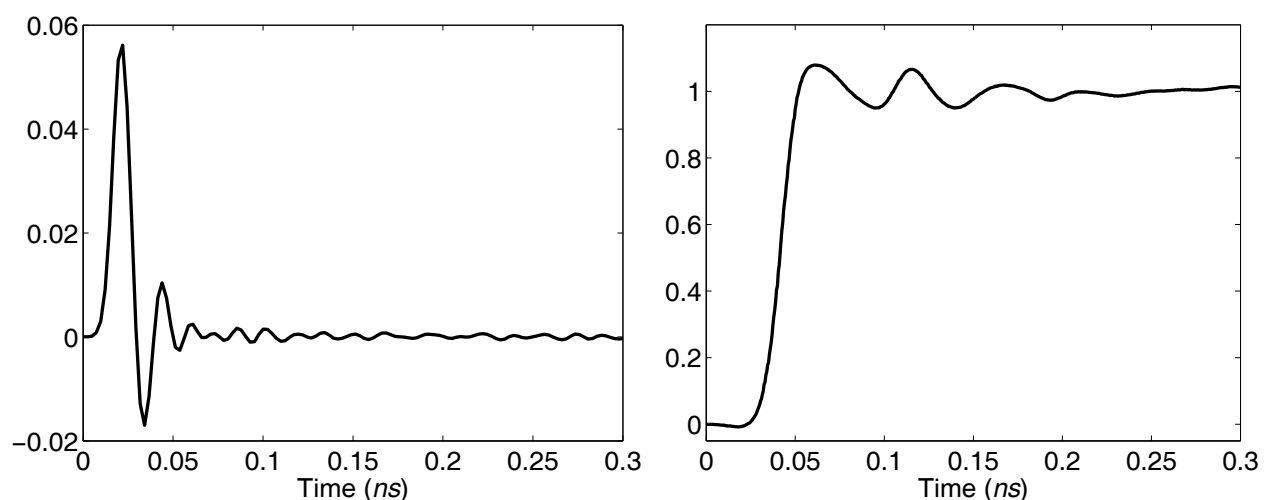


Fig. 3. Example measurement of an optoelectronic pulse with a sampling oscilloscope (left) as described in Clement et al., 2006, and measurement of a voltage step generator with a different calibrated oscilloscope (right).

4.2 System identification

System identification refers here to the estimation of parametric models and their uncertainty (Pintelon & Schoukens, 2001), even though the subject also includes non-parametric methods (Ljung, 1999). To adapt the basic procedure of identifying a model from the experimental characterization (section 4.1) to metrology, follow these steps:

1. Choose a criterion for comparing experimental and modelled characterization.
2. Select a structure for the dynamic model of the measurement. Preferably the choice is based on physical modelling and prior knowledge. General 'black-box' rather than physical models should be utilized for complex systems.
3. Find the numerical values of all model parameters:
 - a. Choose method of optimization.
 - b. Assign start values to all parameters.
 - c. Calculate the hypothetical characterization for the dynamic model.
 - d. Compare experimental and modelled characterization using the criterion in step 1.
 - e. Adjust the parameters of the dynamic model according to step 3a.
 - f. Repeat from c until there is no further improvement in step 3d.
4. Evaluate the performance of the dynamic model by studying the model mismatch.
5. Repeat from step 2 until the performance evaluation in step 4 is acceptable.
6. Propagate the measurement uncertainty of the characterization measurement to the uncertainty of the dynamic model.

There are some important differences in this approach compared to the standard procedure of system identification (Ljung, 1999). Validation of the model is an important step for assessing the correctness of the model, but validation in the conventional sense is here omitted. The reason for this is that it requires at least two characterization experiments to form independent sets of data, one for 'identification' and another for 'validation'. Often only one type of experimental characterization of acceptable accuracy is available. It is then unfortunately impossible to validate the model against data. This serious deficiency is to some extent compensated for by a more detailed concept of measurement uncertainty. The correctness of the model is expressed through the uncertainty of the model, rather than validated by simulations against additional experimental data. All relevant sources of uncertainty should be estimated in the preceding step of characterization, and then propagated to the dynamic model in the last step (6) of identification. Corresponding propagation of uncertainty is indeed discussed in the field of system identification, but perhaps not in the widest sense. The suggested approach is a pragmatic adaptation of well developed procedures of system identification to the concepts of metrology.

The dynamic model is very often non-linear in its parameters (not to be confused with linearity in response!). This is the case for any infinite-impulse response (IIR) pole-zero model. Measurement noise and modelling errors of a large complex model might result in many local optima in the comparison (step 3d). Obtaining convergence of the numerical search may be a challenge, even if the model structure is valid. Assigning good start values to the parameters (step 3b) and limiting the variation in the initial iterations (step 3e), might be crucial. The model may also be identified and extended sequentially (step 2) using the intermediate results as start values for the new model. A sequential approach of this kind is seldom the fastest alternative but often remarkably robust.

A common criterion (step 1) for identifying the parameters is to minimize the weighted square of the mismatch. For frequency response characterization and a symmetric positive definite weighting matrix $W(\omega_k, \omega_l)$, the estimated parameters $\{\hat{q}\}$ are expressed in the residual $\Delta H(q, i\omega_k)$ defined as the difference between modelled and measured response (T represents transposition and $*$ complex conjugation),

$$\{\hat{q}\} = \arg \min_q [\Delta H(q)^T * W \Delta H(q)]. \quad (2)$$

4.2.1 Modelling dynamic measurements

Dynamic models are never true or false, but more or less useful and reliable for the intended use. The primary goal is to strongly reduce the complexity of the characterization to the much lower complexity of a comparatively small model. The difference between the dimensionality of the characterization and the model determines the confidence of the evaluation in step 4. The maximum allowed complexity of the model for acceptable quality of evaluation can be roughly estimated from the number of measured points of the characterization. For a general linear dynamic measurement the model consists of one or several differential (CT: continuous time) or difference (DT: discrete time) equations relating the (input) quantity $x(t)$ to be measured and the measured (output) signal $y(t)$,

$$\begin{aligned} \text{CT: } \quad & \tilde{a}_0 y + \tilde{a}_1 \partial_t y + \tilde{a}_2 \partial_t^2 y + \dots + \tilde{a}_n \partial_t^n y = \tilde{b}_0 x + \tilde{b}_1 \partial_t x + \tilde{b}_2 \partial_t^2 x + \dots + \tilde{b}_m \partial_t^m x \\ \text{DT: } \quad & a_0 y_k + a_1 y_{k-1} + a_2 y_{k-2} + \dots + a_n y_{k-n} = b_0 x_k + b_1 x_{k-1} + b_2 x_{k-2} + \dots + b_m x_{k-m} \end{aligned} \quad (3)$$

where $x_k = x(kT_s)$, $y_k = y(kT_s)$, $k = 0, 1, 2, \dots$, T_s being the sampling time. In both cases it is often convenient to use a state-space formulation (Ljung, 1999), with a system of model equations linear in the differential (CT) or translation (DT) operator. State space equations also allow for multiple input multiple output (MIMO) systems. The related model equation (Eq. 3) can easily and uniquely be derived from any state space formulation. Thus, assuming a model equation of this kind is natural and general. This is very important since it provides a unified treatment of the majority of LTI models used in various applications for describing physical processes, control operations and CT/DT signal processing etc.

An algebraic model equation in the transform variable s or z is obtained by applying the Laplace s -transform to the CT model or the z -transform to the DT model in Eq. 3,

$$\begin{aligned} \text{CT: } \quad & (\tilde{a}_0 + \tilde{a}_1 s + \tilde{a}_2 s^2 + \dots + \tilde{a}_n s^n) Y(s) = (\tilde{b}_0 + \tilde{b}_1 s + \tilde{b}_2 s^2 + \dots + \tilde{b}_m s^m) X(s) \\ \text{DT: } \quad & (a_0 + a_1 z^{-1} + a_2 z^{-2} + \dots + a_n z^{-n}) Y(z) = (b_0 + b_1 z^{-1} + b_2 z^{-2} + \dots + b_m z^{-m}) X(z) \end{aligned} \quad (4)$$

These relations are often expressed in terms of transfer functions $H(s) = Y(s)/X(s)$ or $G(z) = Y(z)/X(z)$. The polynomials are often factorized into their roots, 'zeros' (numerator) and 'poles' (denominator). Another option is to use physical parameters. In electrical circuits lumped resistances, capacitances and inductances are often preferred, while in mechanical applications the corresponding elements are damping, mass and spring constants. In the examples, the parameterization will be a variable number of poles and zeroes. The

fundamental reason for this choice is that it provides not only a very general and effective, but also widely used and understood parameterization. Good initial values of the parameters are in many cases fairly easy to assign by studying the frequency response, and it is straight-forward to extend any model and identify it sequentially.

4.2.2 Uncertainty of dynamic model

The performance of the identified model (step 4) can be explored by studying the properties of the residual $\Delta H(\hat{q}, i\omega_k)$. If the model captures all features of the characterization, the autocorrelation functions of the residual and the measurement noise are similar. For instance, they should both decay rapidly if the measurement noise is uncorrelated (white).

There are many symmetries between the propagation of uncertainty from the characterization to the model (step 6), and from the model to the targeted measurement (section 4.5.1), see Fig. 1. The two propagations will therefore be expressed similarly. The concept of sensitivity is widely used in metrology, and will be utilized in both cases. Just as in section 4.5.1, measured signals must be real-valued, which requires the use of real-valued projections $\varphi(\Delta q, q)$ of the pole and zero deviations Δq (Hessling, 2009a). The deviation in modelled characterization for a slight perturbation φ is given by, $-E^T(\hat{q}, i\omega)\varphi(\Delta q, \hat{q})$ (compare Eq. 12). The matrix $E(\hat{q}, i\omega)$ of sampled sensitivity systems organized in rows is represented in the frequency domain, since the characterization is assumed to consist of frequency response functions. Row n of this matrix is given by $E_n(\hat{q}, i\omega)$ in Eq. 18. The minus sign reflects the fact that the propagation from the characterization to the model is the inverse of the propagation from the model to the correction of the targeted measurement. If the measured characterization deviates by an amount $\Lambda(i\omega)$ from its ensemble mean, the estimated parameters will deviate from their ensemble mean according to $\hat{\varphi}$,

$$\{\hat{\varphi}\} = \arg \min_{\varphi \in \mathcal{R}} \left[(\Lambda^{T*} + \varphi^T E^*) W (\Lambda + E^T \varphi) \right]. \quad (5)$$

The problem of finding the real-valued projected deviation φ (Eq. 5) closely resembles the estimation of all parameters q of the dynamic model (Eq. 2). The optimization over $\varphi \in \mathcal{R}$ is constrained, but much simpler as the model of deviation is linear. Contrary to the problem of non-linear estimation, the linear deviations due to perturbed characterizations can be found explicitly; $\hat{\varphi} = -\text{Re}(\Gamma \Lambda)$, $\Gamma \equiv \left[\text{Re}(E^* W E^T) \right]^{-1} E^* W$. From this solution, the covariance of all projections is readily found ($\langle \cdot \rangle$ denotes average over an ensemble of measurements and let $\hat{\varphi} \rightarrow \varphi$),

$$\langle \varphi \varphi^T \rangle = \frac{1}{2} \text{Re} \left[\Gamma \langle \Lambda \Lambda^T \rangle \Gamma^T + \Gamma \langle \Lambda \Lambda^{T*} \rangle \Gamma^{T*} \right]. \quad (6)$$

This expression propagates the covariance of the characterization experiment $\langle \Lambda \Lambda^{T(*)} \rangle$ to $\langle \varphi \varphi^T \rangle$, which is related to the covariance of the estimated dynamic model. Within the field of system identification (Pintelon & Schoukens, 2001) similar expressions are used, but with sensitivities denoted Jacobians. If the model is accurate the residual is unbiased and reflects

the uncertainty of the characterization, $\langle \Lambda \Lambda^{T(*)} \rangle = \langle \Delta H \Delta H^{T(*)} \rangle - \langle \Delta H \rangle \langle \Delta H^{T(*)} \rangle \approx \langle \Delta H \Delta H^{T(*)} \rangle$. Otherwise there are systematic errors of the model and the residual is biased, $\langle \Delta H \rangle \neq 0$. Not only the covariance of the characterization experiment but also the systematic errors of the identified model should be propagated to the uncertainty. The systematic error $\langle \Delta H \rangle$ can however not be expressed in the model or its uncertainty, as that is how the residual ΔH is defined. A separate treatment according to section 4.3 is thus required: A general upper bound of the dynamic error $\langle \Delta H \rangle$ valid for the targeted measurement should be added directly and *linearly* to the final uncertainty of the targeted measurement (Hessling, 2006).

Only one or at most a few realizations of the residual ΔH are known, since the number of available characterizations is limited. Therefore it is difficult to evaluate *ensemble* averages. However, if the residual is 'stationary' (i.e. do not change in a statistical sense) over a frequency interval $\Delta\omega$, the system is ergodic over this interval. The average over an ensemble of experiments can then be exchanged with a restricted mixed average over frequency and just a few ($m \geq 1$) experimental characterizations,

$$\langle \Delta H(i\omega_1) \Delta H^{(*)}(i\omega_2) \rangle \approx \frac{1}{2\alpha m} \sum_{k=1}^m \int_{-\alpha}^{\alpha} \Delta H^{(k)}(i(\omega_1 + \varpi)) \Delta H^{(k,*)}(i(\omega_2 + \varpi)) d\varpi, \quad (7)$$

where $\alpha = (\Delta\omega - |\omega_1 - \omega_2|)/2 > 0$. If the correlation range is less than the interval of stationary residual, $\langle \Delta H(i\omega_1) \Delta H^{(*)}(i\omega_2) \rangle \approx 0$ for $\alpha < 0$, all elements can be estimated.

As model identification requires experimental characterizations, some of the previous examples will be revisited. The comparison of the load cell and the material testing machine models will illustrate a non-trivial relation between the behaviour of the system (machine) and the part (load cell) traditionally assumed most relevant for the accuracy of the targeted measurement. The propagation of uncertainty (Eq. 6) will not be discussed due to limited space, and as it is a mere transformation of numerical numbers.

4.2.3 Example: Models of load cell and material testing machine

Load cells measure the force in mechanical testing machines often used for fatigue testing of materials and structures, see Fig. 4 (left). It is straightforward to characterize the whole machine by means of built-in force actuators and calibration bars equipped with strain-gauges for measuring force. The calibration bar and load cell outputs can then be compared in a calibration experiment. The load cell can also be characterized separately as explained in section 4.1.1. A recent frequency response characterization and identification of a machine and a load cell (Hessling, 2008c) is compared in Fig. 4 (right) and shown in full in Fig. 5. There is no simple relation or scaling between the amplitude and phases of the frequency responses of the load cell and the installed testing machine. Accurate dynamic characterization in situ thus appears to be required.

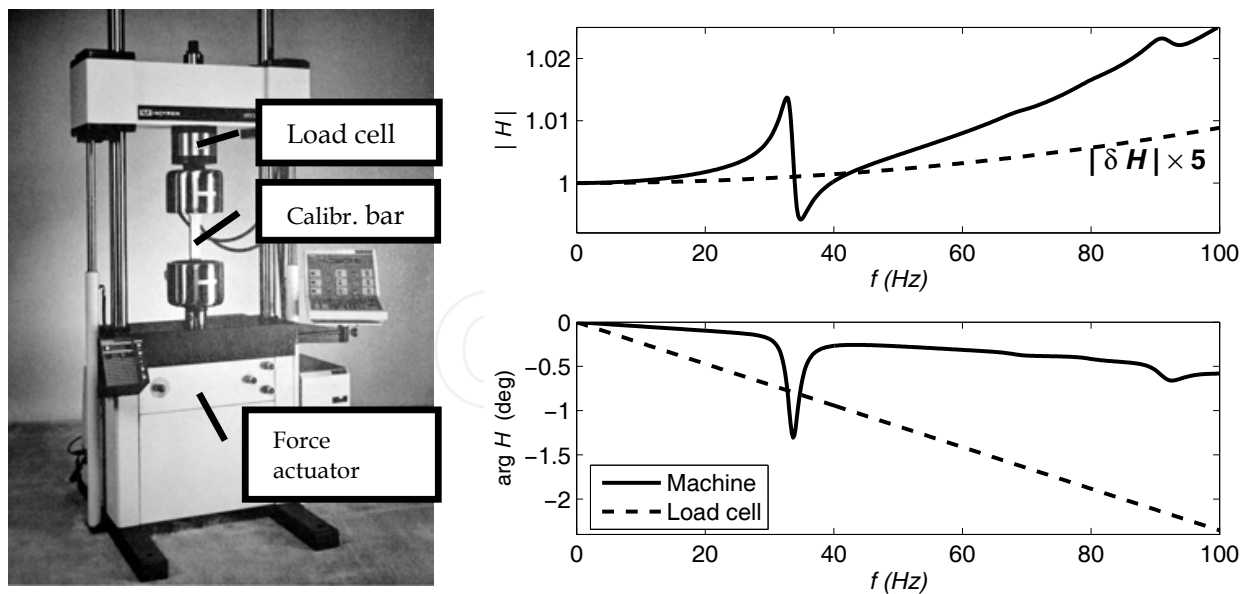


Fig. 4. Magnitude (right, top) and phase (right, bottom) of the frequency response of identified models of a testing machine (left, Table 1: 2*) and its load cell. The legend applies to both figures. The magnitude variation of the load cell is magnified 5 times for clarity.

The autocorrelation of the residual for the load cell (Fig. 6, bottom left) clearly indicates substantial systematic errors. The large residual may be caused by an insufficient dynamic model or a distorted impulse used in the characterization (section 4.1.1). The continuous distribution of mass of the load cell might not be properly accounted for in the adopted lumped model. If the confidence in the model is higher than the random disturbances of the excitation, the residual ΔH may be reduced before propagated to the model uncertainty. Confidence in any model can be formulated as prior knowledge within Bayesian estimation (Pintelon & Schoukens, 2001). The more information, from experiments or prior knowledge, the more accurate and reliable the model will be. However, the fairly complex relation between the machine and the load cell dynamics strongly reduces the need for accurate load cell models. The more important testing machine model is clearly of higher quality (Fig. 6). Pole-zero models of different orders were identified for the testing machine (Table 1). A vibration analysis of longitudinal vibration modes in a state-space formulation (Hessling, 2008c) provided the basic information to set up and interpret these models in terms of equivalent resonance and base resonances. Model 2* is considered most useful.

	Load cell		Machine			
Model (complexity)	-	0	1	2*	3	4
Equiv. resonance (Hz)	2380	635	607	614	616	617
Base resonances (Hz)	-	-	33.7	33.6	33.6	33.6
				91.4	91.3	91.2
					79.6	79.3
						69.3
Weighted residuals ¹	22e-3	48e-4	9.8e-4	6.4e-4	6.4e-4	6.3e-4

Table 1. Identified load cell and material testing machine models. ¹Defined as the root-mean-square of the residuals, divided by the amplification at resonance (load cell), or zero frequency (machine). Not all parameters are displayed (Hessling, 2008c).

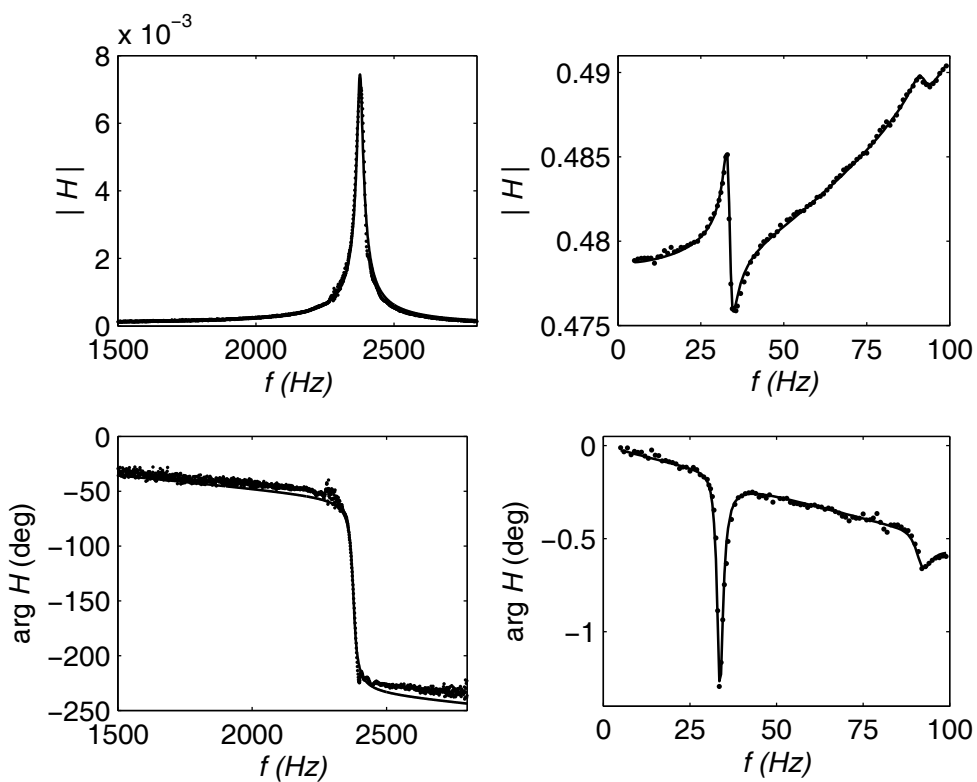


Fig. 5. Model fits for the load cell (left) and the material testing machine (right, Table 1: 2*).

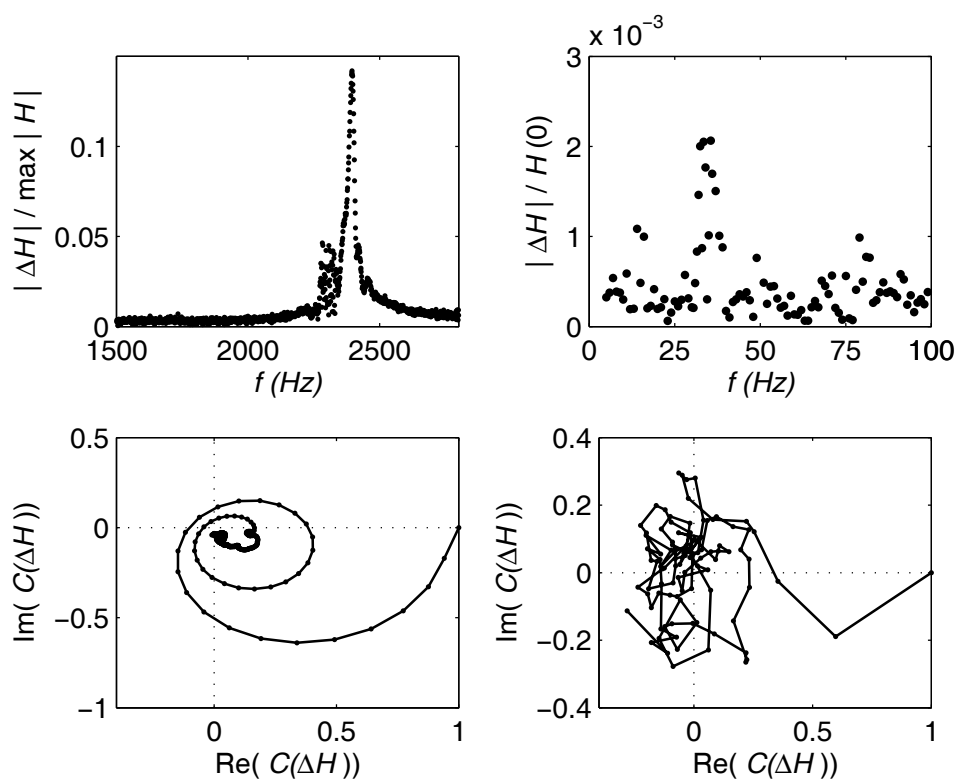


Fig. 6. Magnitude (top) and auto-correlation (bottom) of the residuals ΔH for the load cell (left) and model 2* (Table 1) of the material testing machine (right).

4.2.4 Example: Model of oscilloscope / step generator

The oscilloscope and the generator (section 4.1.2) can be identified in the same manner (Eq. 1). When differentiation is applied, attention has to be paid to noise amplification. It can be mitigated with low-pass filtering. The generator is *modelled* as consisting of an ideal step generator and of a linear time-invariant system which describes all physical limitations. The identified generator model in Fig. 7 may be used to compensate oscilloscope responses for imperfections of the generator. Several corrections for generators and oscilloscopes can be accumulated in a traceability chain and applied in the *final* step of any evaluation, as all operations commute. The model has non-minimum phase (zeros outside the unit circle of the z-plane). This will have consequences for the synthesis of correction (section 4.4.1).

The structure of the generator model could not be derived as it did not correspond to any physical system. Instead, poles and zero were successively added until the residual did not improve significantly. The low resolution of the characterization limited the complexity of possible models. In contrast to the previous example, a discrete rather than continuous time model was utilized for simultaneous identification and discretization in time.

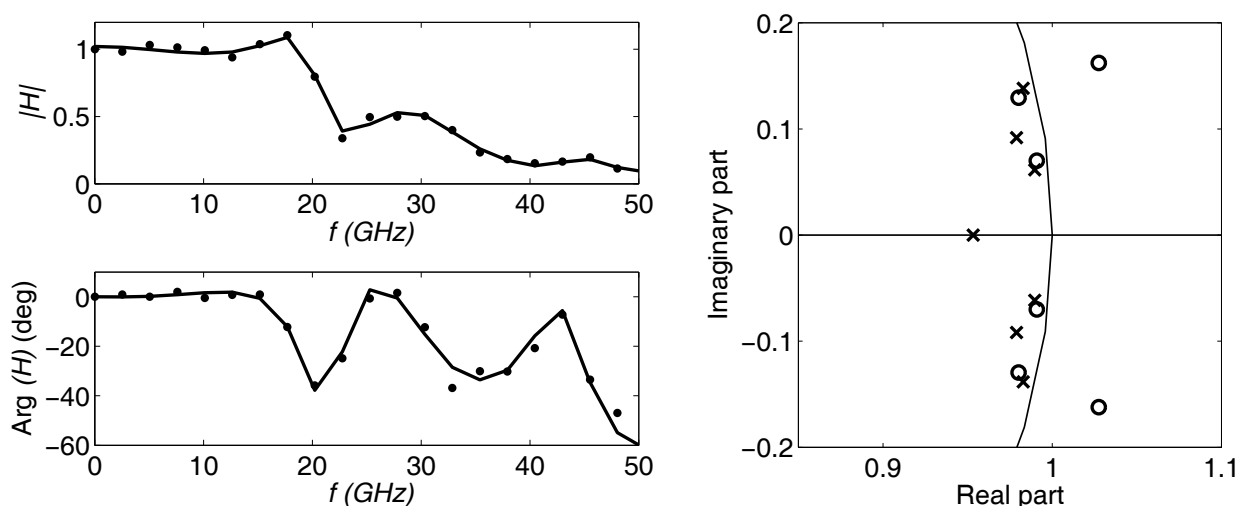


Fig. 7. Magnitude (left, top) and phase (left, bottom) of frequency response functions for an oscilloscope step generator. The characterization (•) is derived from the step response in Fig. 3 (right). The model (line) corresponds to poles and zeros shown in the z-plane (right).

4.3 Systematic error

The dynamic error of a dynamic measurement depends strongly on the variation of the measured signal. The more accurately an error needs to be estimated, the more precise the categorization must be. This manifests a generic problem: To estimate the error with high precision the variation of the physical signal must be well known, but then there would be no need to make a dynamic measurement! Ergo, error estimates are always rather inaccurate. This predicament does however not motivate the common neglect of important error mechanisms (Hessling, 2006). If not taken into account by any means, there is no definite limit to how imprecise the error estimates can be! For substantial correction or precise control though, a low uncertainty of the characterization is an absolute requirement. The concept of dynamic error is intimately related to the perceived time delay. If the time delay is irrelevant it has to be calculated and compensated for when evaluating the error!

Distortion of the signal caused by non-perfect dynamic response of the measurement system makes the determination of the time delay ambiguous. The interpretation of dynamic error influences the deduced time delay. A *joint* definition of the dynamic error and time delay is thus required. The measured signal can for instance be translated in time (the delay) to minimize the difference (the error signal) to the quantity that is measured. The error signal may be condensed with a norm to form a *scalar* dynamic error. Different norms will result in different dynamic errors, as well as time delays. As the error signal is determined by the measurement system, it can be determined from the characterization (section 4.1) or the identified model (section 4.2), and the measured signal.

The norm for the dynamic error should be governed by the measurand. Often it is most interesting to identify an event of limited duration in time where the signal attains its maximum, changes most rapidly and hence has the largest dynamic error. The largest (L^1 norm) relative deviation in the time domain is then a relevant measure. To achieve unit static amplification, normalize the dynamic response $y(t)$ of the measurement system to the excitation $x(t) \in B$. A time delay τ and a relative dynamic error ε can then be defined jointly as (Hessling, 2006),

$$\varepsilon \equiv \min_{\tau} \left[\max_{x(t) \in B, t} \left(\frac{|y(t) - x(t - \tau)|}{\max_t |x(t)|} \right) \right] \cong \min_{\tau} \left(\left\langle \left| \frac{\delta \tilde{H}(i\omega, \tau)}{H(0)} \right| \right\rangle_B \right). \quad (8)$$

$$\langle f \rangle_B \equiv \frac{1}{\omega_B} \int_0^{+\infty} f(\omega) B(\omega) d\omega, \quad \omega_B \equiv \int_0^{+\infty} B(\omega) d\omega$$

The error signal in the time domain is expressed in terms of an error frequency response function $\delta \tilde{H}(i\omega, \tau) \equiv H(\sigma(\omega)) \cdot \exp(i\omega\tau) - H(0)$ related to the transfer function H of the measurement system. The expression applies to both continuous time ($\sigma \rightarrow i\omega$), as well as discrete time systems ($\sigma \rightarrow \exp(i\omega T_s)$), T_s being the sampling time interval). It is advanced in time to adjust for the time delay, in order to give the least dynamic error. The average is taken over the approximated magnitude of the input signal spectrum normalized to one, $B(\omega) \leq 1$, which defines the set B . This so-called *spectral* distribution function (SDF) (Hessling, 2006) enters the dynamic error similarly to how the *probability* distribution function (PDF) enters expectation values. The concept of bandwidth ω_B of the system/signal/SDF is generalized to a 'global' measure insensitive to details of $B(\omega)$ and applicable for any measurement. The error estimate is an upper bound over *all* non-linear phase variations of the excitation as only the magnitude is specified with the SDF. The maximum error signal (x_E) has the non-linear phase $-\delta \tilde{H}(i\omega, \tau)$ and reads (time t_0 arbitrary),

$$\frac{x_E(t)}{\max_t |x_E(t)|} \approx \frac{1}{\omega_B} \int_0^{+\infty} B(\omega) \cos[\omega(t - t_0) - \arg(\delta \tilde{H}(i\omega, \tau))] d\omega. \quad (9)$$

The close relation between the system and the signal is apparent: The non-linear phase of the *system* is attributed to the maximum error *signal* parameterized in properties of the SDF.

The dynamic error and time delay can be visualized in the complex plane (Fig. 8), where the advanced response function $\tilde{H}(i\omega, \tau) = H(\sigma(\omega)) \cdot \exp(i\omega\tau)$ is a phasor 'vibrating' around the positive real axis as function of frequency.

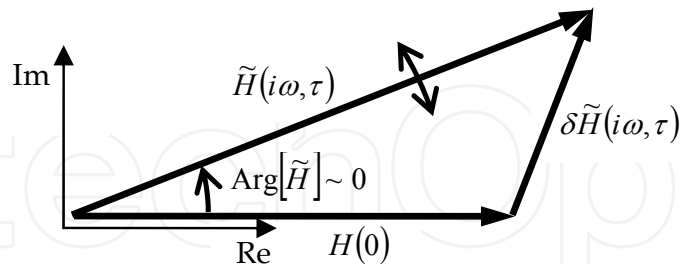


Fig. 8. The dynamic error ε equals the weighted average of $|\delta\tilde{H}(i\omega, \tau)|$ over ω , which in turn is minimized by varying the time delay parameter τ .

For efficient numerical evaluation of this dynamic error, a change of variable may be required (Hessling, 2006). The dynamic error and the time delay is often conveniently parameterized in the bandwidth ω_B and the roll-off exponent of the SDF $B(\omega)$. This dynamic error has several important features not shared by the conventional error bound, based on the amplitude variation of the frequency response within the signal bandwidth:

- The time delay is presented separately and defined to minimize the error, as is often desired for performance evaluation and synchronization.
- All properties of the *signal* spectrum, as well as the frequency response of the measurement *system* are accounted for:
 - The best (as defined by the error norm) linear phase approximation of the measurement system is made and presented as the time delay.
 - Non-linear contributions to the phase are effectively taken into account by removing the best linear phase approximation.
 - The contribution from the response of the system from *outside* the bandwidth of the signals is properly included (controlled by the roll-off of $B(\omega)$).
- A bandwidth of the system can be uniquely defined by the bandwidth of the SDF for which the allowed dynamic error is reached.

The simple all-pass example is chosen to illustrate perhaps the most significant property of this dynamic error - its ability to correctly account for phase distortion. This example is more general than it may appear. Any incomplete dynamic correction of only the magnitude of the frequency response will result in a complex all-pass behaviour, which can be described with cascaded simple all-pass systems.

4.3.1 Example: All-pass system

The all-pass system shifts the phase of the signal spectrum without changing its magnitude. All-pass systems can be realized with electrical components (Ekstrom, 1972) or digital filters (Chen, 2001). The simplest ideal continuous time all-pass transfer function is given by,

$$H(s) = \frac{1 - s/\omega_0}{1 + s/\omega_0} \rightarrow \begin{cases} 1 & s \rightarrow i0 \\ -1 & s \rightarrow i\infty \end{cases} \quad (10)$$

The high frequency cut-off that any physical system would have is left out for simplicity. For slowly varying signals there is only a static error, which for this example vanishes (Fig. 9, top left). The dynamic error defined in Eq. 8 becomes substantial when the pulse-width system bandwidth product increases to order one (Fig. 9, top right), and might exceed 50% (!) (Fig. 9, bottom left). For very short pulses, the system simply flips the sign of the signal (Fig. 9, bottom right). In this case the bandwidth of the system is determined by the curvature of the phase related to $f_0 = \omega_0/2\pi$. The traditional dynamic error bound based on the magnitude of the frequency response vanishes as it ignores the phase! The dynamic error is solely caused by different delays of different frequency components. This type of signal degradation is indeed well-known (Ekstrom, 1972). In electrical transmission systems, the same dispersion mechanism leads to “smeared out” pulses interfering with each other, limiting the maximum speed/bandwidth of transmission.

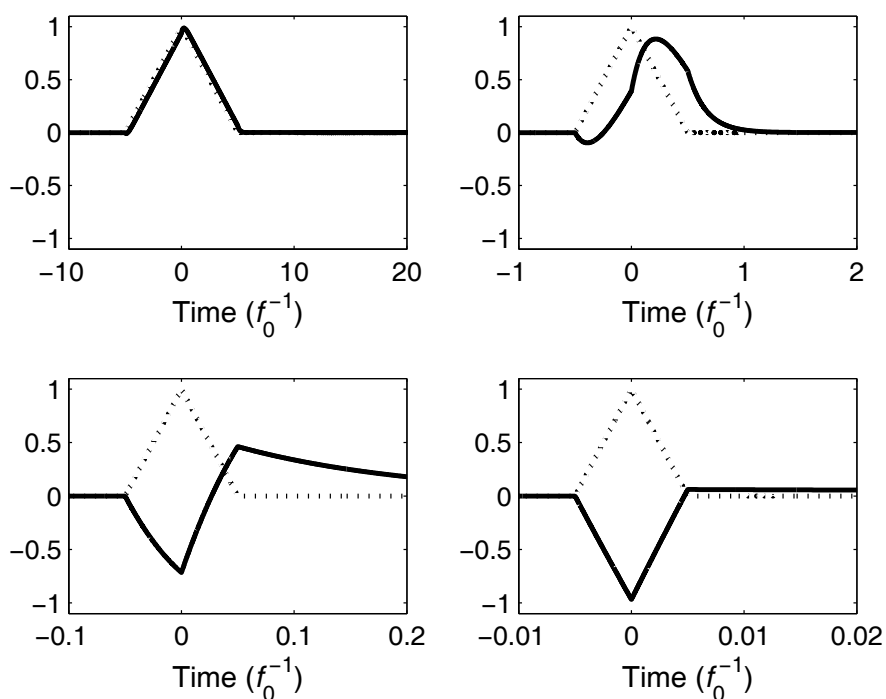


Fig. 9. Simulated measurement (solid) of a triangular pulse (dotted) with the all-pass system (Eq. 10). Time is given in units of the inverse cross-over frequency f_0^{-1} of the system.

Estimated error bounds are compared to calculated dynamic errors for simulations of various signals in Fig. 10. The utilization f_B/f_0 is much higher than would be feasible in practice, but is chosen to correspond to Fig. 9. The SDFs are chosen equal to the magnitude of the Bessel (dotted) and Butterworth (dashed, solid) low-pass filter frequency response functions. Simulations are made for triangular (\diamond), Gaussian (\circ), and low-pass Bessel-filtered square pulse signals ($+$, \square). The parameter n refers to both the order of the SDFs as well as the orders of the low-pass Bessel filters applied to the square signal (FiltSqr). The dynamic error bound varies only weakly with the type (Bessel/Butterworth) of the SDFs: the Bessel SDF renders a slightly larger error due to its initially slower decay with frequency. As expected, the influence from the asymptotic roll-off beyond the bandwidths is very strong. The roll-off in the frequency domain is governed by the regularity or differentiability in the time domain. Increasing the order of filtering (n) of the square pulses (FiltSqr) results in a more regular signal, and hence a lower error. All test signals have strictly linear phase as they are symmetric. The simulated dynamic errors will therefore only reflect the non-linearity of the phase of the system while the estimated error bound also accounts for a possible non-linear phase of the signal. For this reason, the differences between the error bounds and the simulations are rather large.

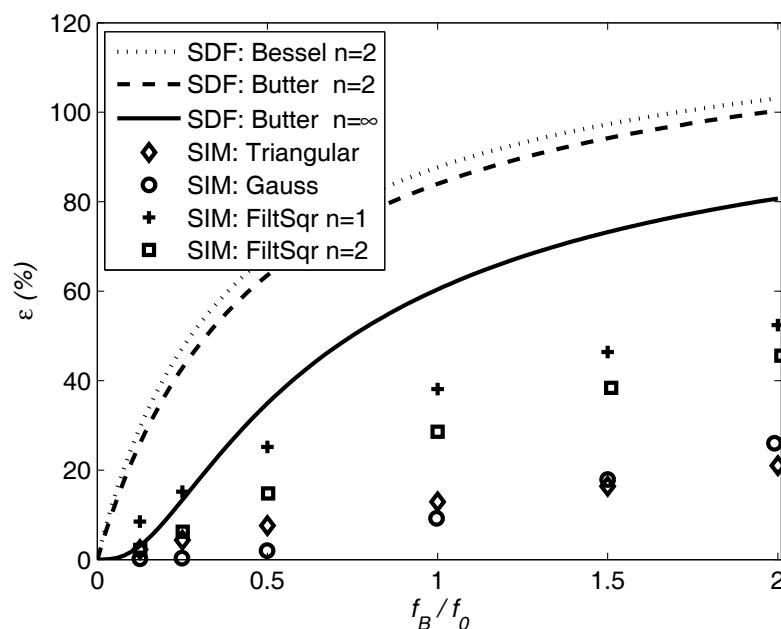


Fig. 10. Estimated dynamic error bounds (lines) for the all-pass system and different SDFs, expressed as functions of bandwidth, compared to simulated dynamic errors (markers).

4.4 Correction

Restoration, de-convolution (Wiener, 1949), estimation (Kailath, 1981; Elster et al., 2007), compensation (Pintelon et al., 1990) and correction (Hessling 2008a) of signals all refer to a more or less optimal dynamic correction of a measured signal, in the frequency or the time domain. In perspective of the large dynamic error of ideal all-pass systems (section 4.3.1), dynamic correction should never even be considered without knowledge of the phase response of the measurement system. In the worst case attempts of dynamic correction result in doubled, rather than eliminated error.

The goals of metrology and control theory are similar, in both fields the difference between the output and the input of the measurement/control system should be as small as possible. The importance of phase is well understood in control theory: The phase margin (Warwick, 1996) expresses how far the system designed for negative feed-back (error reduction - stability) operates from positive feed-back (error amplification - instability). If dynamic correction of any measurement system is included in a control system it is important to account for its delay, as it reduces the phase margin. Real-time correction and control must thus be studied jointly to prevent a potential break-down of the whole system! All internal mode control (IMC)-regulators synthesize dynamic correction. They are the direct equivalents in feed-back control to the type of sequential dynamic correction presented here (Fig. 11).

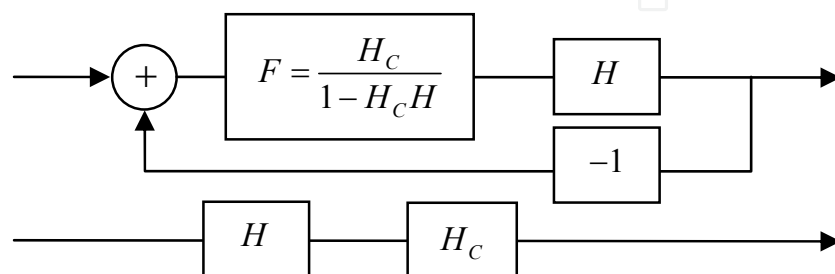


Fig. 11. The IMC-regulator F (top) in a closed loop system is equivalent to the direct sequential correction $H_C \approx H^{-1}$ (bottom) of the [measurement] system H proposed here.

Regularization or noise filtering is required for all types of dynamic correction, H_C must not (metrology) and can not (control) be chosen identical to the inverse H^{-1} . Dynamic corrections must be applied differently in feed-back than in a sequential topology. The sequential correction H_C presented here can be translated to correction within a feed-back loop with the IMC-regulator structure F . Measurements are normally analyzed afterwards (post-processing). That is never an option for control, but provides better and simpler ways of correction in metrology (Hessling 2008a). Causal application should always be judged against potential 'costs' such as increased complexity of correction and distortion due to application of stabilization methods etc.

Dynamic correction will be made in two steps. A digital filter is first synthesized using a model of the targeted measurement. This filter is then applied to all measured signals. Mathematically, measured signals are corrected by propagating them 'backwards' through the modelled measurement system to their physical origin. The synthesis involves inversion of the identified model, taking physical and practical constraints into account to find the optimal level of correction. Not surprisingly, time-reversed filtering in post-processing may be utilized to stabilize the filter. Post-processing gives additional possibilities to reduce the phase distortion, as well as to eliminate the time delay.

The synthesis will be based on the concept of filter 'prototypes' which have the desirable properties but do not always fulfil all constraints. A sequence of approximations makes the prototypes realizable at the cost of increased uncertainty of the correction. For instance, a time-reversed infinite impulse response filter can be seen as a prototype for causal application. One possible approximation is to truncate its impulse response and add a time delay to make it causal. The distortion manifests itself via the truncated tail of the impulse

response. The corresponding frequency response can be used to estimate the dynamic error as in section 4.3. This will estimate the error of making a non-causal correction causal. Decreasing the acceptable delay increases the cost. If the acceptable delay exceeds the response time, there is no cost at all as truncation is not needed.

The discretization of a continuous time digital filter prototype can be made in two ways:

1. Minimize the numerical discrepancy between the characterization of a digital filter prototype and a comparable continuous time characterization for
 - a. a calibration measurement
 - b. an identified model
2. Map parameters of the identified continuous time model to a discrete time model by means of a unique transformation.

Alternative 1 closely resembles system identification and requires no specific methods for correction. In 1b, identification is effectively applied twice which should lead to larger uncertainty. The intermediate modelling reduces disturbances but this can be made more effectively and directly with the choice of filter structure in 1a. As it is generally most efficient in all kinds of 'curve fitting' to limit the number of steps, repeated identification as in 1b is discouraged. Indeed, simultaneous identification and discretization of the system as in 1a is the traditional and best performing method (Pintelon et al., 1990). Using mappings as in 2 (Hessling 2008a) is a very common, robust and simple method to synthesize any type of filter. In contrast to 1, the discretization and modelling errors are disjoint in 2, and can be studied separately. A utilization of the mapping can be defined to express the relation between its bandwidth (defined by the acceptable error) and the Nyquist frequency. The simplicity and robustness of a mapping may in practice override the cost of reduced accuracy caused by the detour of continuous time modelling. Alternative 2 will be pursued here, while for alternative 1a we refer to methods of identification discussed in section 4.2 and the example in section 4.4.1.

As the continuous time prototype transfer function H^{-1} for dynamic correction of H is unphysical (improper, non-causal and ill-conditioned), many conventional mappings fail. The simple exponential pole-zero mapping (Hessling, 2008a) of continuous time $(\tilde{p}_k, \tilde{z}_k)$ to discrete time (p_k, z_k) poles and zeros can however be applied. Switching poles and zeros to obtain the inverse of the transfer function of the original measurement system this transformation reads (T_S the sampling time interval),

$$\begin{aligned} z_k &= \exp(\tilde{p}_k T_S) \\ p_k &= \exp(\tilde{z}_k T_S) \end{aligned} \quad (11)$$

To stabilize and to cancel the phase, the reciprocals of unstable poles and zeros outside the unit circle in the z-plane are first collected in the time-reversed filter, to be applied to the time-reversed signal with exchanged start and end points. The remaining parameters build up the other filter for direct application forward in time. An additional regularizing low-pass noise filter is required to balance the error reduction and the increase of uncertainty (Hessling, 2008a). It will here be applied in both time directions to cancel its phase. For causal noise filtering, a symmetric linear phase FIR noise filter can instead be chosen.

4.4.1 Example: Oscilloscope step generator

From the step response characterization of a generator (Fig. 3, right), a non-minimum phase model was identified in section 4.2.4 (Fig. 7, right). The resulting prototype for correction is unstable, as it has poles outside the unit circle in the z -plane. It can be stabilized by means of time-reversal filtering, as previously described. In Fig. 12, this correction is applied to the original step signal. As expected (EA-10/07), the correction reduces the rise time T about as much as it increases the bandwidth.

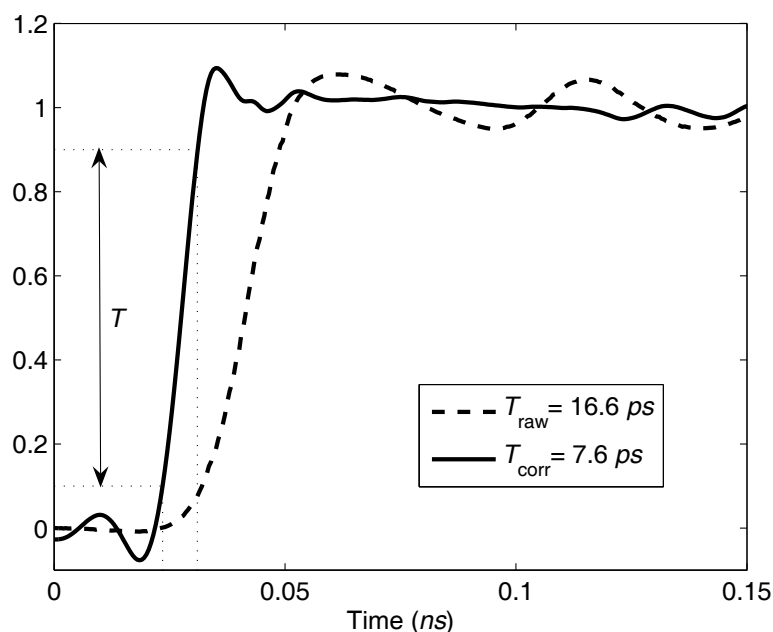


Fig. 12. Original (dashed) and corrected (full) response of the oscilloscope generator (Fig. 3).

Two objections can be made to this result: 1. No expert on system identification would identify the model and validate the correction against the same data. 2. The non-causal oscillations before the step are distinct and appear unphysical as all physical signals must be causal. The answer to both objections is the use of an extended and more detailed concept of measurement uncertainty in metrology, than in system identification: (1) Validation is made through the uncertainty analysis where all relevant sources of uncertainty are combined. (2) The oscillations before the step must therefore be 'swallowed' by any relevant measure of time-dependent measurement uncertainty of the correction.

The oscillations (aberration) are a consequence of the high frequency response of the [corrected] measurement system. The aberration is an important figure of merit controlled by the correction. Any distinct truncation or sharp localization in the frequency domain, as described by the roll-off and bandwidth, must result in oscillations in the time domain. There is a subtle compromise between reduction of rise time and suppression of aberration: Low aberration requires a shallow roll-off and hence low bandwidth, while short rise time can only be achieved with a high bandwidth. It is the combination of bandwidth and roll-off that is essential (section 4.3). A causal correction requires further approximations. Truncation of the impulse response of the time-reversed filter is one option not yet explored.

4.4.2 Example: Transducer system

Force and pressure transducers as well as accelerometers ('T') are often modelled as single resonant systems described by a simple complex-conjugated pole pair in the s-plane. Their usually low relative damping may result in 'ringing' effects (Moghisi, 1980), generally difficult to reduce by other means than using low-pass filters ('A'). For dynamic correction the s-plane poles and zeros of the original measurement system can be mapped according to Eq. 11 to the z-plane shown in Fig. 13. As this particular system has minimum phase (no zeros), no stabilization of the prototype for correction is required. A causal correction is directly obtained if a linear phase noise filter is chosen (Elster et al. 2007). Nevertheless, a standard low-pass noise filter was chosen for application in both directions of time to easily cancel its contribution to the phase response completely.

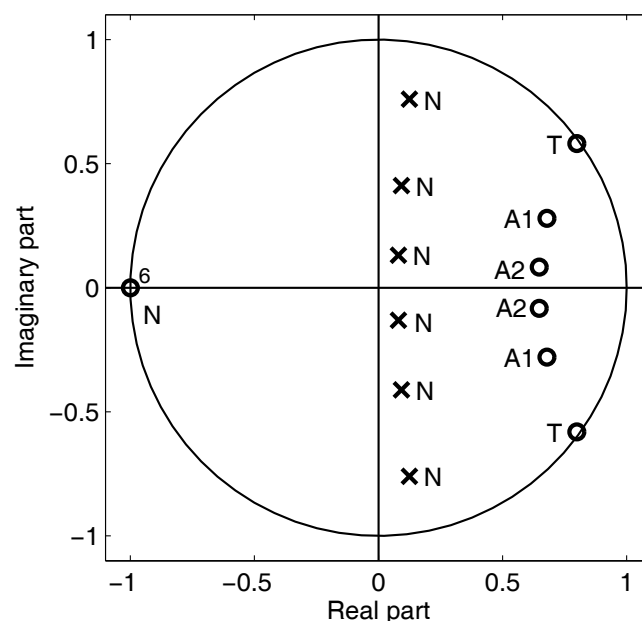


Fig. 13. Poles (x) and zeros (o) of the correction filter: cancellation of the transducer (T) as well as the analogue filter (A), and the noise filter (N).

The system bandwidth after correction was mainly limited by the roll-off of the original system, and the assumed signal-to-noise ratio (50dB). In Fig. 14 (top) the frequency response functions up to the noise filter cut-off, and the bandwidths defined by 5% amplification error before (β) and after (α) correction are shown. This bandwidth increased 65%, which is comparable to the REq-X system (Briel&Kjaer, 2006). The utilization of the maximum 6dB bandwidth set by the cross-over frequency of the noise filter was as high as $\eta = 93\%$. This ratio approaches 100% as the sampling rate increases further and decreases as the noise level decreases. The noise filter cut-off was chosen $f_N = 2f_A$, where f_A is the cross-over frequency of the low-pass filter. The performance of the correction filter was verified by a simulation (Matlab), see Fig. 14 (bottom). Upon correction, the residual dynamic error (section 4.3) decreased from 10% to 6%, the erroneous oscillations were effectively suppressed and the time delay was eliminated.

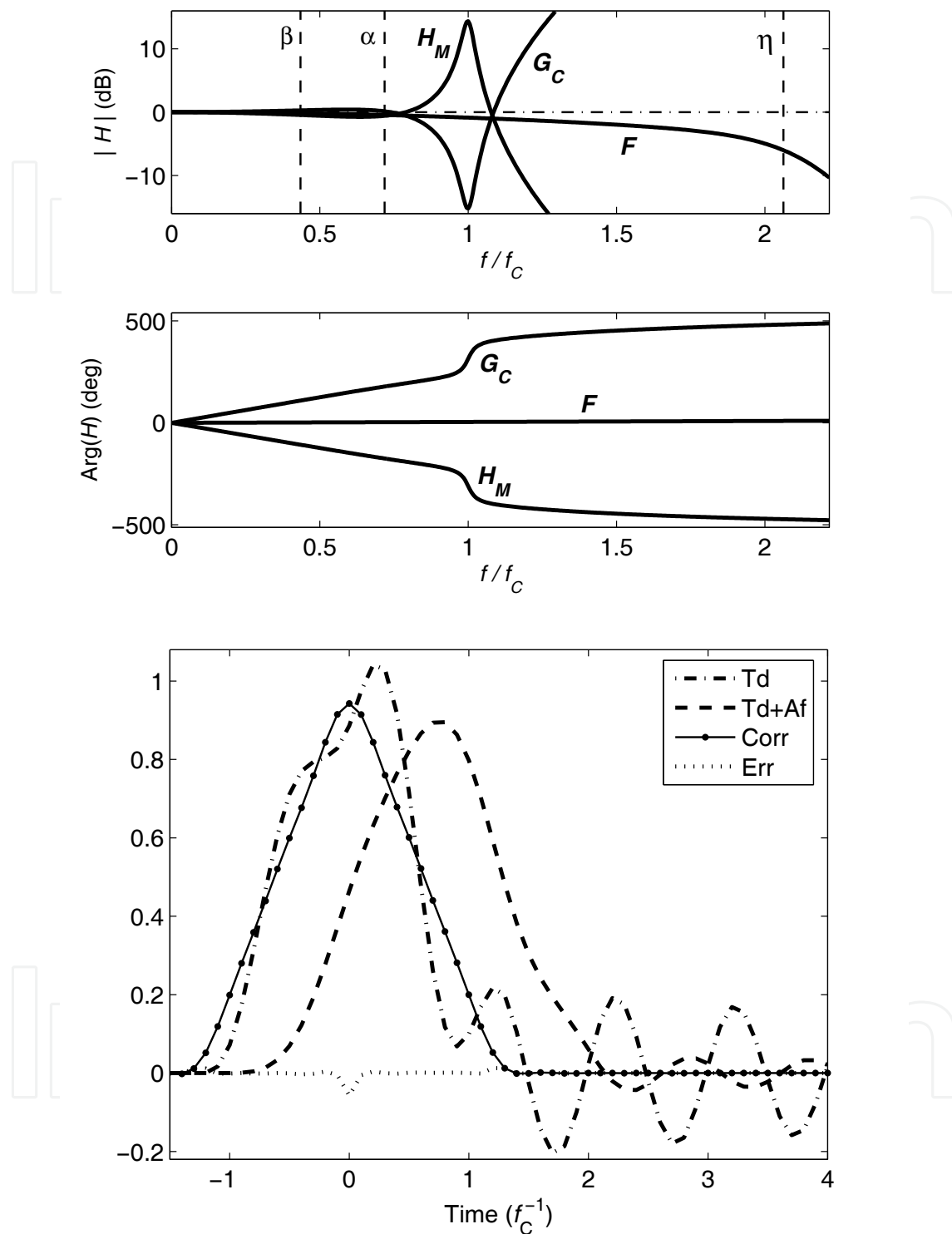


Fig. 14. Magnitude (top) and phase (middle) of frequency response functions for the original measurement system (H_M), the correction filter (G_C) and the total corrected system (F), and simulated correction of a triangular pulse (bottom): corrected signal (Corr), residual error (Err), and transducer signal before (T_d) and after ($T_d + A_f$) the analogue filter. Time is given in units of the inverse resonance frequency f_C^{-1} of the transducer.

4.5 Measurement uncertainty

Traditionally, the uncertainty given by the calibrator is limited to the calibration experiment. The end users are supposed to transfer this information to measurements of interest by using an uncertainty budget. This budget is usually a simple spreadsheet calculation, which at best depends on a most rudimentary classification of measured signals. In contrast, the measurement uncertainty for non-stationary signals will generally have a strong and complex dependence on details of the measured signal (Elster et al. 2007; Hessling 2009a). The interpretation and meaning of uncertainty is identical for all measurements – the uncertainty of the conditions and the experimental set up (input variables) results in an uncertainty of the estimated quantity (measurand). The unresolved problems of non-stationary uncertainty evaluation are not conceptual but practical. How can the uncertainty of input variables be expressed, estimated and propagated to the uncertainty of the estimated measurand? As time and ensemble averages are different for non-ergodic systems such as non-stationary measurements, it is very important to state whether the uncertainty refers to a constant or time-dependent variable. In the latter case, also temporal correlations must be determined. Noise is a typical example of a fluctuating input variable for which both the distribution and correlation is important. If the model of the system correctly catches the dynamic behaviour, its uncertainty must be related to constant parameters. The lack of repeatability is often used to estimate the stochastic contribution to the measurement uncertainty. The uncertainty of non-stationary measurements can however *never* be found with repeated measurements, as variations due to the uncertainty of the measurement or variations of the measurand cannot even in principle be distinguished.

The uncertainty of applying a dynamic correction might be substantial. The stronger the correction, the larger the associated uncertainty must be. These aspects have been one of the most important issues in signal processing (Wiener, 1949), while it is yet virtually unknown within metrology. The guide (ISO GUM, 1993, section 3.2.4) in fact states that “it is assumed that the result of a measurement has been corrected for all recognized significant systematic effects and that every effort has been made to identify such effects”. Interpreted literally, this would by necessity lead to measurement uncertainty without bound. Also, as stated in section 4.4.1 the correction of the oscilloscope generator in Fig. 12 only makes sense (causality) if a relevant uncertainty is associated to it. This context elucidates the pertinent need for reliable measures of non-stationary measurement uncertainty.

The contributions to the measurement uncertainty will here be expressed in generalized time-dependent sensitivity *signals*, which are equivalent to the traditional sensitivity constants. The sensitivity signals are obtained by convolving the generating signals with the virtual *sensitivity systems* for the measurement. The treatment here includes one further step of unification compared to the previous presentation (Hessling, 2009a): The contributions to the uncertainty from measurement noise and model uncertainty are evaluated in the same manner by introducing the concept of generating signals. Digital filters or software simulators will be proposed tools for convolution. Determining the uncertainty of input variables is considered to be a part of system identification (section 4.2.2), assumed to precede the propagation of dynamic measurement uncertainty addressed here.

The measurement uncertainty signal is generally *not* proportional to the measured signal. This typical dynamic effect does not imply that the system is non-linear. Rather, it reveals that the sensitivity systems differ fundamentally from the measurement system.

4.5.1 Expression of measurement uncertainty

To evaluate the measurement uncertainty (ISO GUM, 1993), a model equation is required. For a dynamic measurement it is given by the differential or difference equation introduced in the context of system identification (section 4.2). Also in this case it will be convenient to use the corresponding transformed algebraic equations (Eq. 4), preferably given as transfer functions parameterized in poles and zeros, or physical parameters.

The measurement uncertainty is associated to the quantity of interest contained in the model equation. For measured uncorrected signals, the uncertainty is probably strongly dominated by systematic errors (section 4.3). The model equation for correction is the inverse model equation/transfer function for the direct measurement, adjusted for approximations and modifications required to realize the correction. Generally, a system analysis (Warwick, 1996) of the measurement and all applied operations will provide the required model. For simplicity, this section will only address random contributions to the measurement uncertainty associated to the dynamic correction discussed in section 4.4.

The derivation of the expression of uncertainty in dynamic measurements will be similar for CT and DT, due to the identical use of poles and zeros. Instead of using the inverse Laplace and z-transform, the expressions will be convolved in the time domain with digital filters or dynamic simulators. The propagation of uncertainty from the characterization to the model (section 4.2.2), and from the model to the correction of the targeted measurement discussed here will be evaluated analogously; the model equation or transfer function will be linearized in its parameters and the uncertainty expressed through sensitivity signals. For an efficient model only a few weakly correlated parameters are required. The covariance matrix is in that case not only small but also sparse. As the number of sensitivity signals scales with the size of this matrix, the propagation of uncertainty will be simple and efficient.

The time-dependent deviation χ of the signal of interest from its ensemble mean can be expressed as a matrix product between the deviations φ of all m variables from their ensemble mean, and matrix ξ of all sensitivity signals organized in rows,

$$\chi = \xi^T \varphi, \quad \varphi \equiv (\varphi_1 \quad \varphi_2 \quad \cdots \quad \varphi_m)^T, \quad \xi_{nk} = (e_n * \mu_n)_k. \quad (12)$$

The sensitivity signal ξ_{nk} for parameter φ_n , evaluated at time t_k , is calculated as a convolution (*) between the impulse response e_n of the sensitivity system E_n and a generating signal μ_n . Both the response e_n and the signal μ_n are generally unique for every parameter. In contrast to the previous formulation (Hessling, 2009a), the vector φ here represents *all* uncertain input variables, noise (δy) as well as static and dynamic model parameters (q). The covariance of the error signal is found directly from this expression by squaring and averaging ($\langle \cdot \rangle$) over an ensemble of measurements,

$$\langle \chi \chi^T \rangle = \xi^T \langle \varphi \varphi^T \rangle \xi. \quad (13)$$

The variance or squared uncertainty at different times are given by the diagonal elements of $\langle \chi \chi^T \rangle$. The matrix $\langle \varphi \varphi^T \rangle$ and columns of ξ is the covariance matrix of input variables and sensitivity at a given time often written as (ISO GUM, 1993) $u(x, x)$ and c , respectively.

The combination of Eq. 6 and Eq. 13 propagates the uncertainty of the characterization (Λ) to any time domain measurement (χ) in two steps via the model (Fig. 1), directly (ξ) or indirectly (Γ) via the sensitivity systems E . Physical constraints are fulfilled for all realizations of equivalent measurements (φ), for the parameterization (poles, zeros), and for all representations (frequency and time domain).

The covariance matrix $\langle \varphi\varphi^T \rangle$ will usually be sparse, since different types of variables (such as noise (u_N^2) and model parameters (u_D^2), as well as disjoint subsystems ($u_{D1}^2, u_{D2}^2, \dots, u_{Dn}^2$) characterized separately) usually are uncorrelated,

$$\langle \varphi\varphi^T \rangle = \begin{pmatrix} u_N^2 & 0 \\ 0 & u_D^2 \end{pmatrix}, \quad u_D^2 = \begin{pmatrix} u_{D,1}^2 & 0 & 0 & 0 \\ 0 & u_{D,2}^2 & 0 & 0 \\ 0 & 0 & \ddots & \vdots \\ 0 & 0 & \cdots & u_{D,n}^2 \end{pmatrix}. \quad (14)$$

For each source of uncertainty, the following has to be determined from the model equation:

- a. Uncertain parameter φ_n .
- b. Sensitivity system $E_n(z)$, or $E_n(s)$.
- c. Generating signal for evaluating sensitivity, $\mu_n(t)$.

The presence of measurement noise $\delta y(t)$ is equivalent to having a signal source without control in the transformed model equation (Eq. 4). It is thus trivial that the noise propagates through the dynamic correction $\hat{G}^{-1}(z)$ just like the signal itself, $\delta \hat{X}(z) = \hat{G}^{-1}(z)\delta Y(z)$:

- a. The uncertain parameters are the noise levels at different times, $\varphi_n = \delta y_n = \delta y(t_n)$.
- b. The sensitivity system is identical to the estimated correction, $E_n(z) = \hat{G}^{-1}(z)$.
- c. The sensitivity signal is simply the impulse response of the correction, $\xi_{nk} = \hat{g}_{k-n}^{-1}$.
The generating signal¹ is thus a delta function, $\mu_{nk} = \delta_{nk}$.

The contribution due to noise to the covariance of the corrected signal at different times is directly found using Eq. 13,

$$u_N^2 = (\hat{g}^{-1})^T \langle \delta y \delta y^T \rangle \hat{g}^{-1}. \quad (15)$$

The covariance matrix $\langle \delta y \delta y^T \rangle$ will be band-diagonal with a width set by the correlation time of the noise. This time is usually very short as noise is more or less random. The band of $\langle \delta y \delta y^T \rangle$ is widened by the impulse response \hat{g}^{-1} , as it is propagated to u_N^2 . The matrix u_N^2 is thus also band-diagonal, but with a width given by the sum of the correlation times of the noise and the impulse response \hat{g}^{-1} of the correction. Evidently, not only the probability

¹ The introduction of generating signals may appear superfluous in this context. Nevertheless, it provides a completely *unified* treatment of noise and model uncertainty which greatly simplifies the general formulation. In addition, the concept of generating signals provides more freedom to propagate any obscure source of uncertainty.

distributions but also the temporal correlations of the noise and the uncertainty of the correction are different.

If the noise is independent of time in a statistical sense, it is stationary. In that case the covariance matrix will only depend on the time difference of the arguments, $\langle \delta y_l \delta y_k \rangle = u_Y^2 \cdot \lambda_{|k-l|}$, and thus has a diagonal structure (lines indicate equal elements),

$$\langle \delta y \delta y^T \rangle = u_Y^2 \cdot \begin{pmatrix} \lambda_0 & \lambda_1 & \lambda_2 & \dots \\ \lambda_1 & \lambda_0 & \lambda_1 & \dots \\ \lambda_2 & \lambda_1 & \lambda_0 & \dots \\ \vdots & \vdots & \vdots & \ddots \end{pmatrix}. \quad (16)$$

Further, if the noise is not only stationary but also uncorrelated (white), $\lambda_k = \delta_{k0}$. Only the diagonal will be non-zero. The noise will in this case propagate very simply,

$$u_N^2 = (\hat{g}^{-1})^T \hat{g}^{-1} u_Y^2, \quad \text{diag}[(\hat{g}^{-1})^T \hat{g}^{-1}] = \|\hat{g}^{-1}\|^2 \equiv c_N^2. \quad (17)$$

The variance given by $u_N^2 = c_N^2 u_Y^2$ is as required time-independent since the source is stationary. The sensitivity c_N to stationary uncorrelated measurement noise is simply given by the quadratic norm of the impulse response of the correction.

The propagation of model uncertainty is more complex, because model variations propagate in a fundamentally different manner from noise. Direct linearization will give,

$$\delta H^{-1}(s) H(s) = \sum_n \frac{q_n}{H^{-1}} \frac{\partial H^{-1}}{\partial q_n} \frac{\delta q_n}{q_n} = \sum_n \frac{\partial \ln H^{-1}}{\partial \ln q_n} \frac{\delta q_n}{q_n} \equiv \sum_n E_n(q, s) \frac{\delta q_n}{q_n}. \quad (18)$$

Logarithmic derivatives are used to obtain relative deviations of the parameters and to find simple sensitivity systems $E_n(q, s)$ of low order. Therefore, the generating signals are the corrected rather than the measured signals. This difference can be ignored for a minor correction, as the accuracy of evaluating the uncertainty then is less than the error of calculation.

If the model parameters $\{q_n\}$ are physical:

- a. The uncertain parameters can be the relative variations, $\varphi_n = \delta q_n / q_n$.
- b. The sensitivity systems are $E_n(q, s)$.
- c. The generating signals are all given by the corrected measured signal, $\mu_{nk} = \hat{x}(t_k)$.

For non-physical parameterizations all implicit constraints must be properly accounted for. Poles and zeros are for instance completely correlated in pairs as any measured signal must be real-valued. This correlation could of course be included in the covariance matrix $\langle \varphi \varphi^T \rangle$. A simpler alternative is to remove the correlation by redefining the uncertain parameters. The generating signals $\mu_{nk} = \hat{x}(t_k)$ remain, but the sensitivity systems change accordingly (Hessling, 2009a) (\bullet denotes scalar vector/inner product in the complex s- or z-plane):

- a. For complex-valued pairs of poles and zeros, two projections can be used as uncertain parameters, $\rho_r(q_n) = [\delta q_n / |q_n|] \bullet [q_n^r / |q_n|^r]$, $r = 1, 2$. For all real-valued poles and zeros q the variations can still be chosen as $\varphi_n = \delta q_n / q_n$.
- b. The sensitivity systems can be written as $E_q^{(mn)}(\hat{s}) = \hat{s}^m / (q/|q| - \hat{s})(|q|/q - \hat{s})^{n-1}$, $E_q^{11}(s/|q|)$ for real-valued and $-E_q^{22}(s/|q|)$ and $E_q^{12}(s/|q|)$ for the projections $\rho_1(q)$ and $\rho_2(q)$ of complex-valued pairs of poles and zeros, respectively.

Non-physical parameters require full understanding of implicit requirements but may yield expressions of uncertainty of high generality. Large, complex and different types of measurement systems can be evaluated with rather abstract but structurally simple analyses. Physical parameterizations are highly specific but straight forward to use. The first transducer example uses the general pole-zero parameterization. The second voltage divider example will utilize physical electrical parameters.

The conventional evaluation of the combined uncertainty does not rely upon constant sensitivities. As a matter of fact, the standard quadratic summation of various contributions (ISO GUM, 1993) is already included in the general expression (Eq. 13). The contributions from different sources of uncertainty are added at each instant of time, precisely as prescribed in the GUM for constant sensitivities. The same applies to the proceeding expansion of combined standard uncertainty to any desired level of confidence. In addition, the temporal correlation is of high interest for non-stationary measurement. That is non-trivially inherited from the correlation of the sensitivity signals specific for each measurement, according to the covariance of the uncertain input variables (Eq. 13).

4.5.2 Realization of sensitivity filters

The sensitivity filters are specified completely by the sensitivity systems $E(q, s)$. Filters are generally *synthesized* or constructed from this information to fulfil given constraints. The actual filtering process is *implemented* in hardware or computer programs. The *realization* of sensitivity filters refers to both aspects. Two examples of realization will be suggested and illustrated: digital filtering and dynamic simulations.

The syntheses of digital filters for sensitivity and for dynamic correction described in section 4.4 are closely related. If the sensitivity systems are specified in continuous time, discretization is required. The same exponential mapping of poles and zeros as for correction can be used (Eq. 11). The sensitivity filters for the projections ρ_n will be universal (Hessling, 2009a). Digital filtering will be illustrated in section 4.5.3, for the transducer system corrected in section 4.4.2.

There are many different software packages for dynamic simulations available. Some are very general and each simulation task can be formulated in numerous ways. Graphic programming in networks is often simple and convenient. To implement uncertainty evaluation on-line, access to instruments is required. For post-processing, the possibility to import and read measured files into the simulator model is needed. The risk of making mistakes is reduced if the sensitivity transfer functions are synthesized directly in discrete or continuous time. The Simulink software (Matlab) of Matlab has all these features and will be used in the voltage divider example (Hessling, 2009b) in section 4.5.4.

4.5.3 Example: Transducer system – digital sensitivity filters

The uncertainty of the correction of the electro-mechanical transducer system (section 4.4.2) is determined by the assumed covariance of the model and of the noise given in Table 2.

$u_Y^2 = 50 \text{ dB}$, stationary, uncorrelated ('white')	Measurement noise
$u_M^2 = 10^{-4}$ $\begin{pmatrix} 0.5^2 & 0 & 0 & 0 & 0 & 0 & 0 \\ 0 & 1^2 & 0.1^2 & 0 & 0 & 0 & 0 \\ 0 & 0.1^2 & 0.2^2 & 0 & 0 & 0 & 0 \\ 0 & 0 & 0 & 1^2 & -0.1^2 & 0.05^2 & 0.02^2 \\ 0 & 0 & 0 & -0.1^2 & 0.4^2 & 0.01^2 & -0.03^2 \\ 0 & 0 & 0 & 0.05^2 & 0.01^2 & 1^2 & -0.9^2 \\ 0 & 0 & 0 & 0.02^2 & -0.03^2 & -0.9^2 & 0.8^2 \end{pmatrix}$	Covariance of: static amplification K , transducer (T) and low-pass filter ($A1, A2$) zero projections ρ_1, ρ_2

Table 2. Covariance of the transducer system. The projections ρ_1, ρ_2 are anti-correlated as the zeros approach the real axis (Hessling, 2009a), see entries (6,7)/(7,6) of u_M^2 and Fig. 13.

The cross-over frequency f_N of the low-pass noise filter of the correction strongly affects the sensitivity to noise, $c_N = 36$ for $f_N = 3f_A$ but only $c_N = 2.6$ for $f_N = 2f_A$ (section 4.4.2), where f_A is the low-pass filter cut-off. In principle, the stronger the correction (high cut-off f_N) the stronger the amplification of noise. The model uncertainty increases rapidly at high frequencies because of bandwidth limitations. The systematic errors caused by imperfect discretization in time are negligible if the utilization is high, $\eta \approx 100\%$ (section 4.4.2). The uncertainty in the high frequency range mainly consists of:

1. Residual uncorrected dynamic errors
2. Measurement noise amplified by the correction
3. Propagated uncertainty of the dynamic model

For optimal correction, the uncorrected errors (1) balance the combination of noise (2) and model uncertainty (3). Even though the correction could be maximized up to the theoretical limit of the Nyquist frequency for sampled signals, it should generally be avoided. Rather conservative estimates of systematic errors are advisable, as a too ambitious dynamic correction might do more harm than good. It should be strongly emphasized that the noise level should refer to the *targeted* measurement, not the calibration! As the optimality depends on the measured signal, it is tempting to synthesize adaptive correction filtering related to causal Kalman filtering (Kailath, 1981). With post-processing and a recursive procedure the adaptation could be further improved. This is another example (besides perfect stabilization) of how post-processing may be utilized to increase the performance beyond what is possible for causal correction.

The sensitivity signals for the model are found by first applying the correction filter \hat{g}^{-1} and then the universal filter bank of realized sensitivity systems $E_n(q, z)$ (Eq. 18) (Hessling, 2009a) (omitted for brevity). Three complex-valued pole pairs with two projections, one for the transducer (T) and two for the filter ($A1, A2$, $\text{Im } z_{A1} > \text{Im } z_{A2}$) results in six unique sensitivity signals. For a triangular signal, some sensitivity signals ($T, A1$) are displayed in

Fig. 15 (top). The sensitivities for the transducer and filter models are clearly quite different, while for the two filter zero pairs they are similar (sensitivities for $A2$ omitted). The standard measurement uncertainty u_C in Fig. 15 (bottom) combines noise ($u_Y \rightarrow u_N$) and model uncertainty ($u_M \rightarrow u_D$), see covariance in Table 2. Any non-linear static contribution to the uncertainty has for simplicity been disregarded. To evaluate the expanded measurement uncertainty signal, the distribution of measured values at each instant of time over *repeated measurements* of the *same* triangular signal must be inferred.

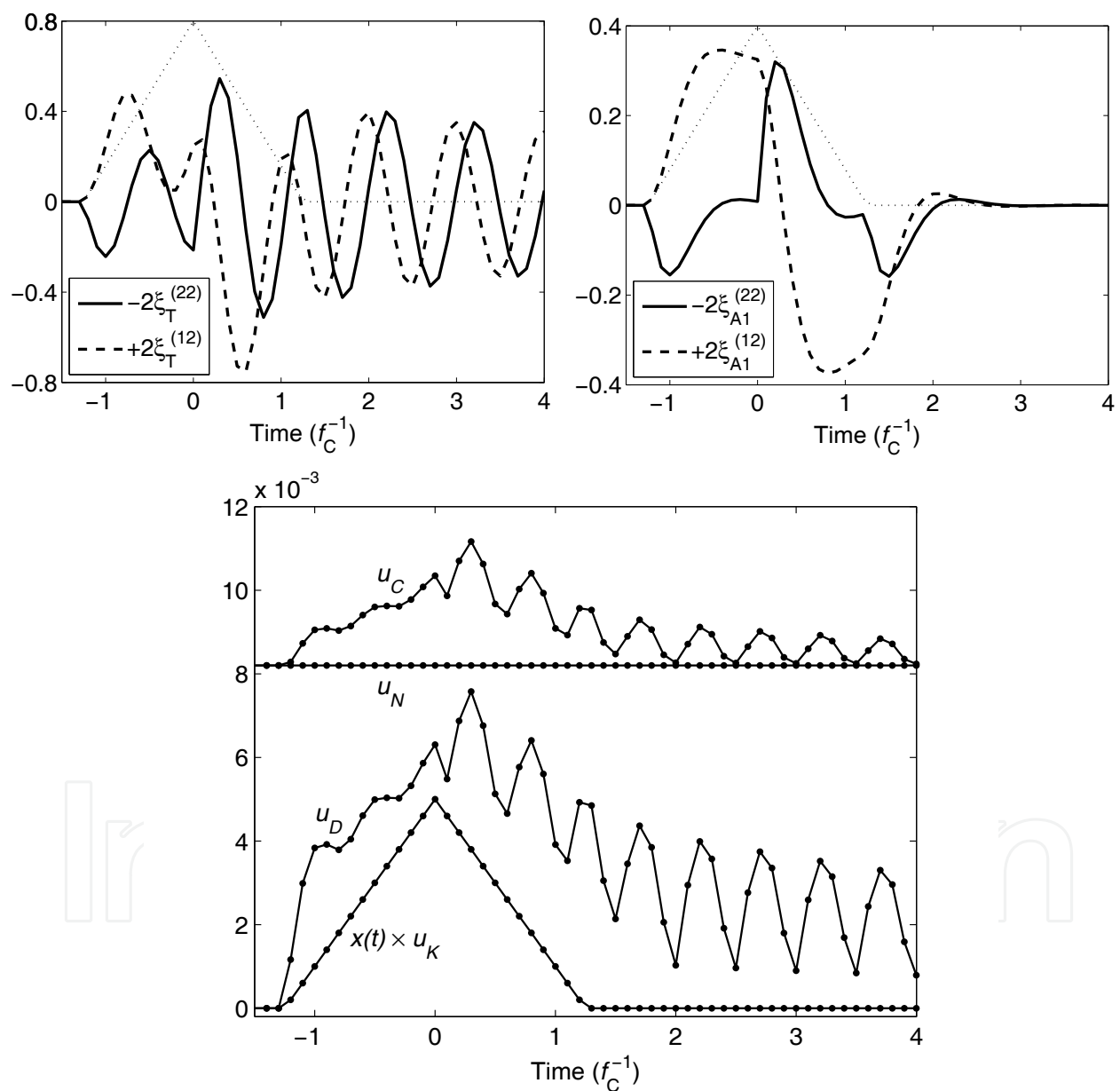


Fig. 15. Measurement uncertainty u_C (bottom) for correction of the electro-mechanical transducer system (Section 4.4.2), and associated sensitivities for the transducer zero pair T projections (top left) and the filter zero pair A1 projections (top right). The measurand (x) (top: dotted, bottom: $u_K \equiv u_M(1,1)$ (Table 2)) is rescaled and included for comparison. Time is given in units of the inverse resonance frequency f_C^{-1} of the transducer.

4.5.4 Example: Voltage divider for high voltage – simulated sensitivities

Voltage dividers in electrical transmission systems are required to reduce the high voltages to levels that are measurable with instruments. Essentially, the voltage divider is a gearbox for voltage, rather than speed of rotation. The equivalent scheme for a capacitive divider is shown in Fig. 16. The transfer function/model equation is found by the well-known principle of voltage division,

$$H(s) = K \frac{1 + (RC)_{LV} s + (LC)_{LV} s^2}{1 + (RC)_{HV} s + (LC)_{HV} s^2}, \quad K = \frac{C_{HV}}{C_{LV}} \ll 1. \quad (19)$$

Linearization of H in $K, R_1, R_2, L_1, L_2, C_1, C_2$ yields seven different sensitivity systems which can be realized directly in Simulink by graphic programming (Fig. 17).

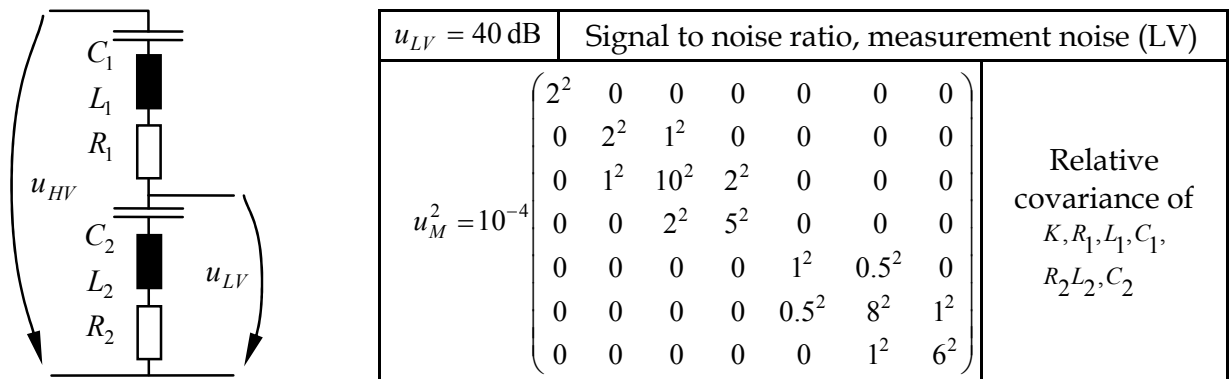


Fig. 16. Electrical model of capacitive voltage divider for high voltage (left) with covariance (right). The high (low) voltage input (output) circuit parameters are labelled HV (LV).

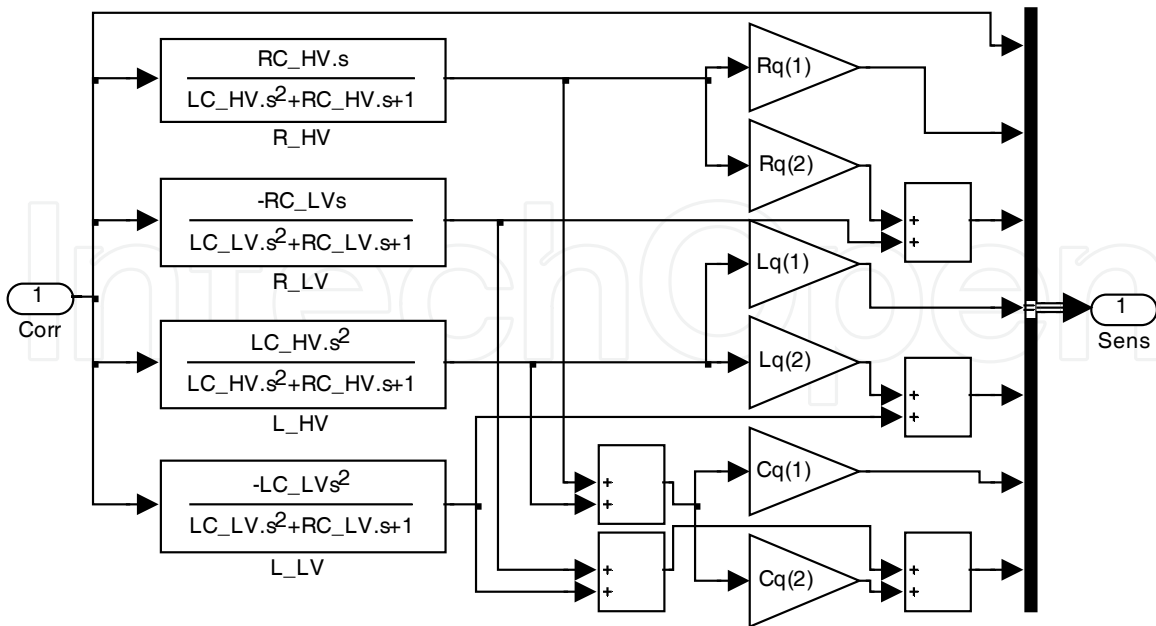


Fig. 17. Simulink model for generating model sensitivity from corrected signals (Corr). Here, $Xq(n) \equiv X_n / X_{HV}$, where $X = \{R, L, C\}$, $n = \{1, 2\}$ and X_{HV} the total for the HV circuit.

As the physical high-frequency cut-off was not modelled (Eq. 19), no noise filter was required. To calculate the noise sensitivity from the impulse response (Eq. 17), proper and improper parts of the transfer function had to be analyzed separately (Hessling, 2009b). In Fig. 18 the uncertainty of correcting a standard lightning impulse (u_{HV}) is simulated. The signal could equally well have been any corrected voltmeter signal, fed into the model with the data acquisition blocks of Simulink. The R, L, C parameters were derived from resonance frequency $f_C = [2.3 \ 0.8]$ MHz and relative damping $\zeta = [1.2 \ 0.4]$ of the HV and LV circuits, and nominal ratio of voltage division $K = 1/1000$. The resulting sensitivities are shown in Fig. 18 (left). The measurement uncertainty of the correction (u_C) in Fig. 18 (right) contains contributions from the noise ($u_{LV} \rightarrow u_N$) and the model ($u_M \rightarrow u_D$).

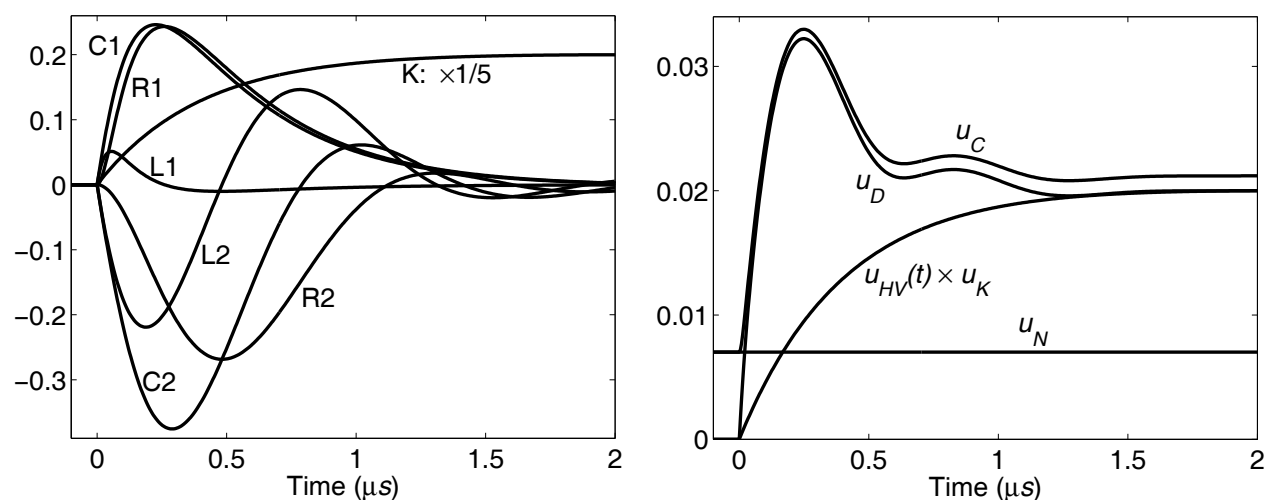


Fig. 18. Model sensitivities ξ (left) for the standard lightning impulse u_{HV} (left: $u_{HV} \propto \xi_K$, right: $u_K = u_M(1,1)$), and measurement uncertainty u_C (right) for dynamic correction.

4.6 Known limitations and further developments

Dynamic Metrology is a framework for further developments rather than a fixed concept. The most important limitation of the proposed methods is that the measurement system must be linear. Linear models are often a good starting point, and the analysis is applicable to all non-linear systems which may be accurately linearized around an operating point.

Even though measurements of non-stationary quantities are considered, the system itself is assumed time-invariant. Most measurement systems have no measurable time-dependence, but the experimental set up is sometimes non-stationary. If the time-dependence originates from outside the measurement system it can be modelled with an additional influential (input) signal.

The propagation of uncertainty has only been discussed in terms of sensitivity. This requires a dynamic model of the measurement, linear in the uncertain parameters. Any obscure correlation between the input variables is however allowed. It is an unquestionable fact that the distributions often are not accurately known. Propagation of uncertainty beyond the concept of sensitivity can thus seldom be utilized, as it requires more knowledge of the distributions than their covariance.

The mappings for synthesis of digital filters for correction and uncertainty evaluation are chosen for convenience and usefulness. The over-all results for mappings and more accurate numerical optimization methods may be indistinguishable. Mappings are very robust, easy to transfer and to illustrate. The utilization ratio of the mapping should be defined according to the noise filter cross-over rather than, as customary, the Nyquist frequency. This fact often makes the mappings much less critical.

The de-facto standard is to evaluate the measurement uncertainty in post-processing mode. Non-causal operations are then allowed and sometimes provide signal processing with superior simplicity and performance. Instead of discussing causality, it is more appropriate to state a maximum allowed time delay. When the ratio of the allowed time delay to the response time of the measurement system is much larger than one, also non-causal operations like time-reversed filtering can be accurately realized in real-time. If the ratio is much less than one, it is difficult to realize any causal operation, irrespectively of whether the prototype is non-causal or not. Finding good approximations to fulfil strong requirements on fast response is nevertheless one topic for future developments.

Finding relevant models of interaction in various systems is a challenge. For analysis of for instance microwave systems this has been studied extensively in terms of scattering matrices. How this can be joined and represented in the adopted transfer function formalism needs to be further studied.

Interpreted in terms of distortion there are many different kinds of uncertainty which need further exploration. The most evident source of distortion is a variable amplification in the frequency domain, which typically smoothes out details. A finite linear phase component is equivalent to a time delay which increases the uncertainty immensely, if not adjusted for. Distortion due to non-linear phase skews or disperses signals. All these effects are presently accounted for. However, a non-linear response of the measurement system gives rise to another type of systematic errors, often quantified in terms of total harmonic distortion (THD). A harmonic signal is then split into several frequency components by the measurement system. This figure of merit is often used e.g. in audio reproduction. Linear distortion biases or colours the sound and reduces space cognition, while non-linear distortion influences 'sound quality'. Non-linear distortion is also discussed extensively in the field of electrical power systems, as it affects 'power quality' and the operation of the equipment connected to the electrical power grid. A concept of non-linear distortion for non-stationary measurements is missing and thus a highly relevant subject for future studies.

5. Summary

In the broadest possible sense *Dynamic Metrology* is devoted to the analysis of dynamic measurements. As an extended calibration service, it contains many novel ingredients currently not included in the standard palette of metrology. Rather, Dynamic Metrology encompasses many operations found in the fields of system identification, digital signal processing and control theory. The analyses are more complex and more ambiguous than conventional uncertainty budgets of today. The important interactions in non-stationary measurements may be exceedingly difficult to both control and to evaluate. In many situations, in situ calibrations are required to yield a relevant result. Providing metrological services in this context will be a true challenge.

Dynamic Metrology is currently divided into four blocks. The calibrator performs the characterization experiment (1) and identifies the model of the measurement (2). The dynamic correction (3) and evaluation of uncertainty (4) are synthesized for *all* measurements by the calibrator, while these steps must be realized by the end user for *every* single measurement. The proposed procedures of uncertainty evaluation for non-stationary quantities closely resemble the present procedure formulated in the Guide to the Expression of Uncertainty in Measurement (ISO GUM, 1993), but its formulation needs to be generalized and exemplified since for instance:

- The sensitivities are generally time-dependent *signals* and not constants.
- The sensitivity is *not* proportional to the measured or corrected signal.
- The uncertainty refers to distributions over *ensembles* and *temporal correlations*.
- The model equation is one or several *differential* or *difference* equation(s).
- The uncertainty, dynamic correction or any other comparable signal is *unique* for every combination of measurement *system* and measured or corrected *signal*.
- Proper estimation of systematic errors requires a robust concept of *time delay*.
- Complete dynamic correction must never be the goal, as noise would be amplified without any definite bound.

6. References

- ASTM E 467-98a (1998). *Standard Practice for Verification of Constant Amplitude Dynamic Forces in an Axial Fatigue Testing System*, The American Society for testing and materials
- Bruel&Kjaer (2006). Magazine No. 2 / 2006, pp. 4-5, <http://www.bksv.com/4279.asp>
- Chen Chi-Tsong (2001). *Digital Signal Processing*, Oxford University Press, ISBN 0-19-513638-1, New York
- Clement, T.S.; Hale, P.D.; Williams, D. F.; Wang, C. M.; Dienstfrey, A.; & Keenan D.A. (2006). Calibration of sampling oscilloscopes with high-speed photodiodes, *IEEE Trans. Microw. Theory Tech.*, Vol. 54, (Aug. 2006), pp. 3173-3181
- Dienstfrey, A.; Hale, P.D.; Keenan, D.A.; Clement, T.S. & Williams, D.F. (2006). Minimum phase calibration of oscilloscopes, *IEEE Trans. Microw. Theory. Tech.* 54 No. 8 (Aug. 2006), pp. 481-491
- EA-10/07, EAL-G30 (1997) *Calibration of oscilloscopes*, edition 1, European cooperation for accreditation of laboratories
- Ekstrom, M.P. (1972). Baseband distortion equalization in the transmission of pulse information, *IEEE Trans. Instrum. Meas.* Vol. 21, No. 4, pp. 510-5
- Elster, C.; Link, A. & Bruns, T. (2007). Analysis of dynamic measurements and determination of time-dependent measurement uncertainty using a second-order model, *Meas. Sci. Technol.* Vol. 18, pp. 3682-3687
- Esward, T.; Elster, C. & Hessling, J.P. (2009) Analyses of dynamic measurements: new challenges require new solutions, *XIX IMEKO World Congress*, Lisbon, Portugal Sept., 2009
- Hale, P. & Clement, T.S. (2008). Practical Measurements with High Speed Oscilloscopes, *72rd ARFTG Microwave Measurement Conference*, Portland, OR, USA, June 2008
- Hessling, P. (1999). Propagation and summation of flicker, *Cigre' session 1999*, Johannesburg, South Africa
- Hessling, J.P. (2006). A novel method of estimating dynamic measurement errors, *Meas. Sci. Technol.* Vol. 17, pp. 2740-2750

- Hessling, J.P. (2008a). A novel method of dynamic correction in the time domain, *Meas. Sci. Technol.* Vol. 19, pp. 075101 (10p)
- Hessling, J.P. (2008b). Dynamic Metrology – an approach to dynamic evaluation of linear time-invariant measurement systems, *Meas. Sci. Technol.* Vol. 19, pp. 084008 (7p)
- Hessling, J.P. (2008c). Dynamic calibration of uni-axial material testing machines, *Mech. Sys. Sign. Proc.*, Vol. 22, 451-66
- Hessling, J.P. (2009a). A novel method of evaluating dynamic measurement uncertainty utilizing digital filters, *Meas. Sci. Technol.* Vol. 20, pp. 055106 (11p)
- Hessling, J.P. & Mannikoff, A. (2009b) Dynamic measurement uncertainty of HV voltage dividers, *XIX IMEKO World Congress*, Lisbon, Portugal Sept., 2009
- Humphreys, D.A. & Dickerson, R.T. (2007). Traceable measurement of error vector magnitude (EVM) in WCDMA signals, *The international waveform diversity and design conference*, Pisa, Italy, 4-8 June 2007
- IEC 61000-4-15 (1997). *Electromagnetic compability (EMC), Part 4: Testing and measurement techniques, Section 15: Flickermeter - Functional and design specifications*, International Electrotechnical commission, Geneva
- ISO 2631-5 (2004). *Evaluation of the Human Exposure to Whole-Body Vibration*, International Standard Organization, Geneva
- ISO 16063 (2001). *Methods for the calibration of vibration and shock transducers*, International Standard Organization, Geneva
- ISO GUM (1993). *Guide to the Expression of Uncertainty in Measurement*, 1st edition, International Standard Organization, ISBN 92-67-10188-9, Geneva
- Kailath, T. (1981). *Lectures on Wiener and Kalman filtering*, Springer-Verlag, ISBN 3-211-81664-X, Vienna, Austria
- Kollár, I.; Pintelon, R.; Schoukens, J. & Simon, G. (2003). Complicated procedures made easy: Implementing a graphical user interface and automatic procedures for easier identification and modelling, *IEEE Instrum. Meas. Magazine* Vol. 6, No. 3, pp. 19-26
- Ljung, L. (1999). *System Identification: Theory for the User*, 2nd Ed, Prentice Hall, ISBN 0-13-656695-2, Upper Saddle River, New Jersey
- Matlab with System Identification, Signal Processing Toolbox and Simulink, The Mathworks, Inc.
- Moghisi, M.; Squire, P.T. (1980). An absolute impulsive method for the calibration of force transducers, *J. Phys. E.: Sci. Instrum.* Vol. 13, pp. 1090-2
- Pintelon, R. & Schoukens, J. (2001). *System Identification: A Frequency Domain Approach*, IEEE Press, ISBN 0-7803-6000-1, Piscataway, New Jersey
- Pintelon, R.; Rolain, Y.; Vandeen Bossche, M. & Schoukens, J. (1990) Toward an Ideal Data Acquisition Channel, *IEEE Trans. Instrum. Meas.* Vol. 39, pp. 116-120
- 3GPP TS (2006). *Tech. Spec. Group Radio Access Network; Base station conformance testing*
- Warwick, K. (1996). *An introduction to control systems*, 2nd Ed, World Scientific, ISBN 981-02-2597-0, Singapore
- Wiener, N. (1949). *Extrapolation, Interpolation, and Smoothing of Stationary Time Series*, Wiley, ISBN 0-262-73005-7, New York
- Williams, D.F.; Clement, T.S.; Hale, P. and Dienstfrey, A. (2006). Terminology for high-speed sampling oscilloscope calibration, *68th ARFTG Microwave Measurement Conference*, Broomfield, CO, USA, Dec. 2006



Advances in Measurement Systems

Edited by Milind Kr Sharma

ISBN 978-953-307-061-2

Hard cover, 592 pages

Publisher InTech

Published online 01, April, 2010

Published in print edition April, 2010

How to reference

In order to correctly reference this scholarly work, feel free to copy and paste the following:

Jan Peter Hessling (2010). Metrology for Non-Stationary Dynamic Measurements, Advances in Measurement Systems, Milind Kr Sharma (Ed.), ISBN: 978-953-307-061-2, InTech, Available from:

<http://www.intechopen.com/books/advances-in-measurement-systems/metrology-for-non-stationary-dynamic-measurements>

INTECH

open science | open minds

InTech Europe

University Campus STeP Ri
Slavka Krautzeka 83/A
51000 Rijeka, Croatia
Phone: +385 (51) 770 447
Fax: +385 (51) 686 166
www.intechopen.com

InTech China

Unit 405, Office Block, Hotel Equatorial Shanghai
No.65, Yan An Road (West), Shanghai, 200040, China
中国上海市延安西路65号上海国际贵都大饭店办公楼405单元
Phone: +86-21-62489820
Fax: +86-21-62489821

intechopen

© 2010 The Author(s). Licensee IntechOpen. This chapter is distributed under the terms of the [Creative Commons Attribution-NonCommercial-ShareAlike-3.0 License](#), which permits use, distribution and reproduction for non-commercial purposes, provided the original is properly cited and derivative works building on this content are distributed under the same license.

IntechOpen

IntechOpen